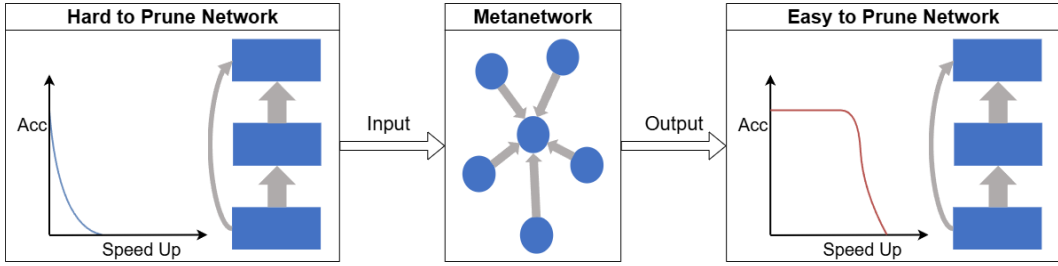


META PRUNING VIA GRAPH METANETWORKS : A UNIVERSAL META LEARNING FRAMEWORK FOR NETWORK PRUNING

006 **Anonymous authors**

007 Paper under double-blind review



020 Figure 1: For a pruning criterion, we use a metanetwork to change a hard to prune network into
021 another easy to prune network for better pruning.

ABSTRACT

025 We propose an entirely new meta-learning framework for network pruning. It
026 is a general framework that can be theoretically applied to almost all types of
027 networks with all kinds of pruning and has great generality and transferability.
028 Experiments have shown that it can achieve outstanding results on many popular
029 and representative pruning tasks (including both CNNs and Transformers). Unlike
030 all prior works that either rely on fixed, hand-crafted criteria to prune in a coarse
031 manner, or employ learning to prune ways that require special training during
032 each pruning and lack generality. Our framework can learn complex pruning
033 rules automatically via a neural network (metanetwork) and has great generality
034 that can prune without any special training. More specifically, we introduce
035 the newly developed idea of metanetwork from meta-learning into pruning. A
036 metanetwork is a network that takes another network as input and produces a
037 modified network as output. In this paper, we first establish a bijective mapping
038 between neural networks and graphs, and then employ a graph neural network
039 as our metanetwork. We train a metanetwork that learns the pruning strategy
040 automatically and can transform a network that is hard to prune into another
041 network that is much easier to prune. Once the metanetwork is trained, our
042 pruning needs nothing more than a feedforward through the metanetwork and
043 some standard finetuning to prune at state-of-the-art. Our code is available at
044 <https://anonymous.4open.science/r/MetaPruning>.

1 INTRODUCTION

045 With the rapid advancement of deep learning (LeCun et al., 2015; Schmidhuber, 2015), neural
046 networks have become increasingly powerful. However, this improved performance often comes
047 with a significant increase in the number of parameters and computational cost (FLOPs). As a result,
048 there is growing interest in methods to simplify these networks while preserving their performance.
049 Pruning, which involves selectively removing certain parts of a neural network, has proven to be an
050 effective approach (Cheng et al., 2024; He & Xiao, 2024; Reed, 1993).

053 A key idea of a large number of previous pruning works is to remove the unimportant components of
a neural network. To achieve this goal, various criteria that measure the importance of components of

054 a neural network have been invented. Some criteria are based on norm or magnitude scores (Han
 055 et al., 2016; Li et al., 2017b; Sun et al., 2024; He et al., 2018a). Some are based on how much the
 056 performance changes when certain parts of the network are removed or preserved (You et al., 2019b;
 057 Ma et al., 2023; Frankle & Carbin, 2019; Ye et al., 2020). Some others defined more complex criteria
 058 such as saliency and sensitivity (LeCun et al., 1989; Lee et al., 2019; Zhao et al., 2019).

059 Once a pruning criterion is established, we can assess whether a model is easy or hard to prune based
 060 on that criterion. Technically, we consider a model easy to prune if we can prune a relatively large
 061 part of it with only little loss in accuracy. Otherwise, we consider it hard to prune.
 062

063 Prior researchers have generally approached pruning improvement in two ways: either by refining the
 064 pruning criteria or by transforming the model to be easier to prune according to a given criterion. The
 065 first approach is more straightforward and has been extensively studied in prior work. In contrast, the
 066 second approach has received comparatively less attention. However, several studies adopting this
 067 latter perspective have achieved promising results. Notably, sparsity regularization methods (Wen
 068 et al., 2016; Fang et al., 2023; Wang et al., 2021) exemplify this approach by encouraging models to
 069 become sparser, thereby facilitating more effective pruning.
 070

071 Our framework inherits the idea of the second way. A metanetwork is a network that takes another
 072 network as input and produces a modefied network as output. For any given pruning criterion, our
 073 framework aims at training a metanetwork that can transform a hard to prune network into another
 074 easier to prune network like figure 1.
 075

076 Our contributions can be summarized as follows:
 077

- 078 (1) Introduce the idea of metanetwork from meta-learning into pruning for the first time.
 079
- (2) Propose an entirely new universal pruning framework that is theoretically applicable
 080 to almost all types of networks with all kinds of pruning.
 081
- (3) Present concrete implementations for our theoretical framework and achieve state-of-
 082 the-art performance on various practical pruning tasks.
 083
- (4) Conduct further research on the flexibility and generality of our framework.
 084

085 Our method is entirely new and fundamentally different from all prior works, see Appendix A for a
 086 comparison with prior works to better understand our novel contributions and advantages.
 087

088 2 RELATED WORK

089 2.1 METANETWORKS

090 Using neural networks to process other neural networks has emerged as an intriguing research
 091 direction. Early studies demonstrated that neural networks can extract useful information directly
 092 from the weights of other networks (Unterthiner et al., 2020). We define a *metanetwork* as a neural
 093 network that takes another neural network as input and outputs either information about it or a
 094 modified network. Initial metanetworks were simple multilayer perceptrons (MLPs), while more
 095 recent designs incorporate stronger inductive biases by preserving symmetries (Godfrey et al., 2022)
 096 inherent in the input networks. Broadly, metanetwork architectures can be categorized into two
 097 perspectives. The *weight space view* applies specially designed MLPs directly on the model’s
 098 weights (Zaheer et al., 2017; Navon et al., 2023; Zhou et al., 2023a; Tran et al., 2024b; Zhou et al.,
 099 2023b; 2024; Tran et al., 2024a). And the *graph view* transforms the input network into a graph and
 100 applies graph neural networks (GNNs) to it (Lim et al., 2024; Kofinas et al., 2024; Kalogeropoulos
 101 et al., 2024). In this work, we adopt the graph view to build our metanetwork, leveraging the natural
 102 correspondence between graph nodes and neurons in a network layer, as well as the symmetries they
 103 exhibit (Maron et al., 2019). Given the maturity and effectiveness of GNNs, the graph metanetwork
 104 approach offers both elegance and practicality.
 105

106 2.2 GRAPH NEURAL NETWORKS

107 Graph neural networks (GNNs) are a class of neural networks specifically designed to operate on
 108 graph-structured data, where graphs consist of nodes and edges with associated features (Wu et al.,
 109 2021; Scarselli et al., 2009; Kipf & Welling, 2017). GNNs have gained significant attention in recent
 110

108 years, with frameworks such as the message passing neural network (MPNN) (Gilmer et al., 2017)
 109 proving to be highly effective. In this paper, we employ the message passing framework, specifically
 110 using Principal Neighborhood Aggregation (PNA) (Corso et al., 2020) as the backbone architecture
 111 for our metanetwork.
 112

113 2.3 SPARSITY REGULARIZATION BASED PRUNING

114 Networks that are inherently sparse tend to be easier to prune effectively. Prior research has explored
 115 various regularization techniques to encourage sparsity in neural networks to facilitate pruning. This
 116 idea of sparsity regularization has been widely adopted across many works (Wen et al., 2016; Gordon
 117 et al., 2018; Huang & Wang, 2018; Lin et al., 2020c; He et al., 2017; Lin et al., 2019; Xia et al., 2022;
 118 2024; Fang et al., 2023; Wang et al., 2021). Our method inherits this principle to some extent, as our
 119 metanetwork can be viewed as transforming the original network into a sparser version for better
 120 pruning.
 121

122 2.4 LEARNING TO PRUNE & META PRUNING

123 Given the complexity of pruning, several previous works have leveraged neural networks (Dery et al.,
 124 2024; He et al., 2017; Wu et al., 2024; Chen et al., 2023), reinforcement learning (Rao et al., 2019;
 125 Yu et al., 2022; He et al., 2018b), and other techniques to automatically learn pruning strategies.
 126 Viewing pruning as a learning problem naturally leads to the idea of meta-learning, which learns
 127 “how to learn” (Hospedales et al., 2022). Some prior works have specifically applied meta-learning to
 128 pruning (Liu et al., 2019; Li et al., 2020). Our work also draws idea from meta-learning, but it learns
 129 in a way entirely different from all prior works.
 130

131 3 A UNIVERSAL META-LEARNING FRAMEWORK

132 Our framework can be summarized in one single sentence (Figure 1):

133 **For a pruning criterion, we use a metanetwork to change a hard to prune**
 134 **network into another easy to prune network for better pruning.**

135 **Pruning criterion:** A pruning criterion measures the importance of specific components of a neural
 136 network. Typical examples include the ℓ_1 norm and ℓ_2 norm of weight vectors. During pruning, we
 137 compute an importance score for each prunable component according to the criterion, and remove
 138 components in ascending order of their scores.

139 **Easy or hard to prune:** For a fixed pruning criterion, if we gradually prune the network and the
 140 accuracy drops quickly, we refer to it as *hard to prune*. Conversely, if the accuracy decreases slowly
 141 with progressive pruning, we call it *easy to prune*.

142 **Metanetwork:** A metanetwork is a special type of neural network whose inputs and outputs are
 143 both neural networks. In contrast, standard neural networks typically take structured data such as
 144 images (CNNs), sentences (Transformers), or graphs (GNNs) as input. A metanetwork, however,
 145 takes an existing network as input and outputs another network, hence the term *meta*—indicating that
 146 it operates on neural networks themselves.

147 4 A SPECIFIC IMPLEMENTATION BASED ON GRAPH METANETWORKS

148 The proposed framework is conceptually simple and straightforward. However, its practical imple-
 149 mentation requires addressing several technical challenges:

- 150 (1) How to build the metanetwork ?
- 151 (2) How to train the metanetwork ?
- 152 (3) How to design the pruning criterion ?

153 We present our implementations step by step, dedicating one subsection to each challenge. The final
 154 subsection offers an overall summary of our method and a deeper understanding of it from a more
 155 holistic perspective.

162
163

4.1 METANETWORK DESIGN

164
165
166
167
168

Drawing ideas from recent researches (section 2.1), we use a graph neural network (GNN) as our metanetwork. Please make sure you are familiar with the basic concepts of GNN before continuing. Our design does not cover any complex GNN theory, you only need to know what is a graph and the basic message passing algorithm.

169
170
171
172
173
174
175

Conversion between networks and graphs: To apply a metanetwork (GNN) on networks, we first need to establish a conversion between networks and graphs. Prior works such as Kofinas et al. (2024); Lim et al. (2024) have managed to change networks of almost all architectures (CNN, Transformer, RNN, etc.) into graphs.

176
177
178
179
180
181
182
183

Here we show how we establish conversion between a ResNet (He et al., 2016) and a graph in our experiments as an example. This inherits the idea of Kofinas et al. (2024); Lim et al. (2024) but is quite different in implementation details. To convert a network into a graph, we establish the correspondence between the components of a neural network and elements of a graph as follows:

184
185
186
187
188
189
190
191
192
193
194
195
196
197
198

(1) **Node:** Each neuron in fully connected layers or channel in convolutional layers in the network is represented as a node in the graph. (2) **Edge:** An edge exists between two nodes if there is a direct connection between them in the original network. This includes fully connected layers, convolutional layers, and residual connections. (3) **Node Features:** Node features comprise parameters associated with neurons, here we use the weight, bias, running mean, running var of batchnorm (Ioffe & Szegedy, 2015), including both batchnorms from previous adjacent layers and previous skip connection layers (if exist). (4) **Edge Features:** Edge features encode the weights of connections between nodes. We treat linear connections and residual connections as special cases of convolutional connections with a kernel size of 1. For a $k \times k$ convolution between two channels, we flatten it into a k^2 -dim edge feature vector.

199
200
201
202

Since graph neural networks here require all edge features to have the same dimension, we adopt one of two strategies to standardize them: (1) Pad all convolutional kernels to the same size (e.g., the maximum kernel size in the network) (2) Flatten convolutional kernels of varying sizes, then apply learned linear transformations to project them into the same size.

203
204
205
206

During conversion, we simply ignored other components such as pooling layers. Although we have methods to explicitly convert all of them, our experiments show that omitting them already yields outstanding results. Therefore, it is acceptable to ignore them in practice. We also didn't use any other techniques like positional embedding.

207
208
209
210
211

By following these rules, we can generate a graph that corresponds to a given neural network. Conversely, the inverse transformation can be applied to convert a graph back into an equivalent network. In essence, we establish an equivalent conversion between networks and graphs. For a more intuitive understanding, see Figure 2.

212
213
214
215

Metanetwork architecture: After establishing the conversion between networks and graphs, we can convert the input network into a graph, use metanetwork(GNN) to transform the graph, and finally convert the output graph back into a new network. Our metanetwork must be powerful enough to learn the transforming rules for better pruning. We build our metanetwork based on the message passing framework (Gilmer et al., 2017) and PNA (Corso et al., 2020) architecture. A brief overview of our architecture is provided below, the full description is available in Appendix B.1.

Conversion between Network and Graph		
Network	Graph	
		$1 \rightarrow 3$: $\begin{bmatrix} -0.7 & 2.9 & -5.3 \\ 4.4 & -9.8 & 1.4 \\ 5.2 & -3.1 & 1.0 \end{bmatrix}$ $\rightarrow 5$: Batchnorms From 3,4 $\begin{bmatrix} 1.3 & -0.4 & 2.2 & 5.1 \end{bmatrix}$ From 1,2 $\begin{bmatrix} -0.6 & 0.9 & -5.6 & 3.1 \end{bmatrix}$
		$1 \rightarrow 3$: Edge Feature $\begin{bmatrix} -0.7 & 2.9 & -5.3 & 4.4 & -9.8 & 1.4 & 5.2 & -3.1 & 1.0 \end{bmatrix}$ 5: Node Feature $\begin{bmatrix} 1.3 & -0.4 & 2.2 & 5.1 & -0.6 & 0.9 & -5.6 & 3.1 \end{bmatrix}$

Figure 2: **Conversion between networks and graphs:** We visualize a two layer toy CNN as example. Our graph contains 6 nodes corresponding with 6 neurons in the network. For neurons connected via convolutional channel like (1,3) and connected by residual connection like (1,5), we add an edge between their corresponding nodes. Then we generate node and edge features as shown in the figure. For some special cases, we use default values to replace non-existent values. For example, for node 3 who doesn't have a residual connection, we set the last 4 number of its node feature as [1, 0, 0, 1]. This means we treat it as with previous residual batchnorm of weight 1, bias 0, running mean 0, running var 1, performing the same as with no batchnorm.

Since graph neural networks here require all edge features to have the same dimension, we adopt one of two strategies to standardize them: (1) Pad all convolutional kernels to the same size (e.g., the maximum kernel size in the network) (2) Flatten convolutional kernels of varying sizes, then apply learned linear transformations to project them into the same size.

During conversion, we simply ignored other components such as pooling layers. Although we have methods to explicitly convert all of them, our experiments show that omitting them already yields outstanding results. Therefore, it is acceptable to ignore them in practice. We also didn't use any other techniques like positional embedding.

216 We use v_i to represent node i 's feature vector, and e_{ij} to represent feature vector of the edge between
 217 i and j . We consider undirected edges, i.e., e_{ij} is the same as e_{ji} . Our metanetwork is as follows.
 218

219 First, all input node and edge features are encoded into the same hidden dimension.

220 $v \leftarrow \text{MLP}_{\text{NodeEnc}}(v_{in}),$ (1)

221 $e \leftarrow \text{MLP}_{\text{EdgeEnc}}(e_{in}).$ (2)

223 Then they will pass through several message passing layers. In each layer, we update node and edge
 224 features using information from adjacent nodes and edges.
 225

226 $v_i \leftarrow f_v(v_i, v_j((i, j) \in E), e_{ij}((i, j) \in E))$ (3)

227 $e_{ij} \leftarrow f_e(v_i, v_j, e_{ij})$ (4)

229 Here f_v and f_e are fixed calculating processes.

230 Finally, we use a decoder to recover node and edge features to their original dimensions:

232 $v_{pred} \leftarrow \text{MLP}_{\text{NodeDec}}(v),$ (5)

233 $e_{pred} \leftarrow \text{MLP}_{\text{EdgeDec}}(e).$ (6)

235 We multiply predictions by a residual coefficient and add them to the original inputs as final outputs:

237 $v_{out} = \alpha \cdot v_{pred} + v_{in},$ (7)

238 $e_{out} = \beta \cdot e_{pred} + e_{in},$ (8)

240 where α and β in practice are set to a small real numbers like 0.01. This design enables the
 241 metanetwork to learn only the delta weights on top of the original weights, instead of a complete
 242 reweighting.

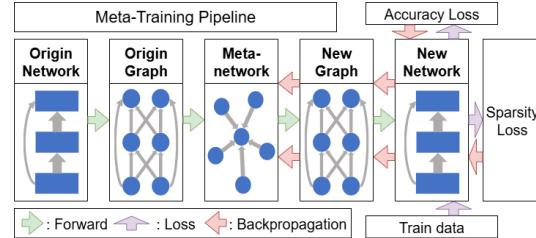
4.2 META-TRAINING

246 Meta-training is the process we train our metanetwork (Figure 3).

247 **Data preparation:** Meta-training data is com-
 248 prised of two parts. The first is a set of neural
 249 networks to prune, which serve as the origin
 250 network in meta-training. We call them *data*
 251 *models*. The number of data models can be ar-
 252 bitrary small numbers like 1, 2, or 8, because
 253 our implementations aren't sensitive to it (See
 254 more explanations in Section 4.4). The second is
 255 the traditional training datasets, CIFAR-10 for
 256 example, used to calculate the accuracy loss.

257 **One training iteration:** We select one model
 258 from data models as the origin network. It is
 259 converted into its graph representation, passed
 260 through the metanetwork to get a new graph
 261 and converted back into a new network. We
 262 calculate accuracy loss and sparsity loss on this
 263 new network, and backpropagated the gradients
 264 to update the metanetwork.

265 Two types of losses are used during meta-training. (1) **Accuracy Loss:** We feed the training data (e.g.,
 266 Train set of CIFAR-10. Note that test set is not used here) into the new network and compute the
 267 cross-entropy loss based on the output predictions, ensuring the metanetwork doesn't excessively
 268 disturbing the effective parts of the origin network. (2) **Sparsity Loss:** We calculate a regularization
 269 term on the new network to encourage it to be sparse, making it easier to prune. It is related to the
 design of pruning criterion (section 4.3)



270 **Figure 3: Meta-Training Pipeline:** During each
 271 iteration, the origin network is converted into the
 272 origin graph, fed through the metanetwork to get
 273 a new graph and finally converted back into a new
 274 network. We calculate accuracy loss and sparsity
 275 loss on the new network, then backpropagated the
 276 gradients to update the metanetwork.

270
271

4.3 PRUNING CRITERION

272
273
274
275

A valid pruning criterion consists of two components: (1) **An importance score function:** During pruning, we calculate the scores of all prunable components of a network, and prune them in ascending order of their scores. (2) **A sparsity loss:** It is a kind of loss that is calculated on the parameters of the network. Optimizing the network using this loss can make it easier to prune.

276
277
278
279

We perform most of our experiments by default using structural pruning, but also include a small number of experiments with unstructured and N:M sparsity pruning to demonstrate that our method can be applied to all kinds of pruning. In unstructured pruning and N:M sparsity pruning, we simply use the naive l_1 norm as both our importance score function and sparsity loss.

280
281
282
283

In structural pruning, we draw ideas from prior sparsity regularization based pruning methods (section 2.3), and design our pruning criterion based on them (especially Fang et al. (2023)). We will give a brief introduction below. For a rigorous mathematical definition and more details, please refer to appendix B.2.

284
285
286
287
288
289

A variant of the classical l_2 norm, the *group norm* is used as our importance score function. It inherits the idea of using l_2 norm to calculate a score, but calculate it on a pruning group level. Since structural pruning is performed on groups, traditional l_2 norm that treats nodes and edges in isolation is no longer viable. Group l_2 norm that takes a whole group into consideration has shown to be more effective. We calculate the sparsity loss by multiply our group norm scores with some coefficients.

290
291
292
293

The choice of pruning criteria is highly flexible (see in our later experiments, section 6.1), which further demonstrates the generality of our framework. We perform most of our experiments by default using structural pruning, but also include a small number of experiments with unstructured and N:M sparsity pruning to demonstrate that our method can be applied to all kinds of pruning.

294
295

4.4 A HOLISTIC PERSPECTIVE

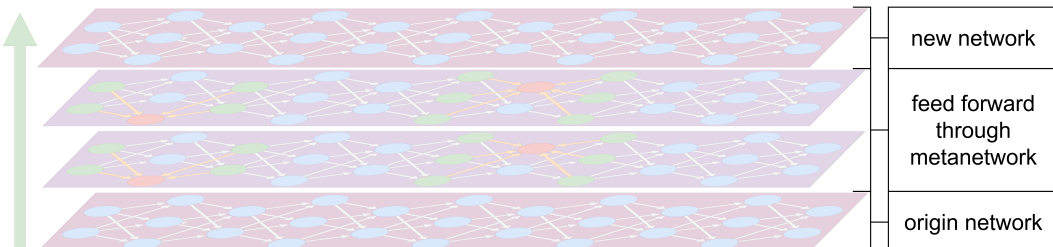
304
305
306

Figure 4: **Feed forward through metanetwork:** when a network is fed forward through the metanetwork, every parameter in it gathers information from neighbour parameters and architectures.

307
308
309
310

Intuitively, when a network is fed forward through the metanetwork, every parameter in it gathers information from neighbour parameters and architectures (Figure 4). The metanetwork automatically learns how to process the information from neighbours and change the weights of the network based on that for better pruning. And this has several important properties:

311
312
313
314
315
316
317
318
319
320

Generality: Our metanetwork is a really small GNN compared to the origin network, which means each parameter can only see information from a limited local region. Due to the nature of GNN, parameters at any position in the network—whether at the beginning, middle, or end—must process information from neighbours in the same way. As a result, the metanetwork must learn a general strategy to adjust parameters based on neighbour information for better pruning. This explains why, in all our experiments, the pruning models and meta-training data models are completely different, but the performance is as good as the same. This also explains why our implementations are not sensitive to the number of data models. Even a single data model can be viewed as a collection of numerous data points sufficient to train the metanetwork. So there is no overfitting at all, and whether we are using 1, 2 or 8 data models during meta-training, the results remain the same.

321
322
323

Natural transferability: Just as a GNN can be applied to graphs of varying sizes without modification, our metanetwork can be directly applied to networks of different scales. This property gives it natural transferability, as demonstrated in our experiments (section 6.3) where it successfully transfers across related datasets and network architectures.

324 **Universally applicability:** Theoretically, our implementations can be applied to almost all types
 325 of networks with all kinds of pruning. Almost all types of networks can be converted into graphs
 326 (Kofinas et al., 2024; Lim et al., 2024), and the designs of the GNN and the pruning criteria are also
 327 broadly compatible. This makes our framework a universally applicable solution for network pruning.
 328

329 5 EXPERIMENTS ON CLASSICAL CNN PRUNING TASKS

330 5.1 PRELIMINARIES

$$333 \quad \underbrace{\text{Initial Pruning (Finetuning)}}_{\text{Optional}} \rightarrow \underbrace{\text{Metanetwork (Finetuning)}}_{\text{Necessary}} \rightarrow \text{Pruning (Finetuning)} \quad (9)$$

336 Definitions of the terms *Speed Up* and *Acc vs. Speed Up Curve* are in Appendix C.1. The pruning
 337 pipeline is described as equation 9, and full details are provided in Appendix C.2.

339 Unlike prior learning to prune methods that require special training during each pruning, our pruning
 340 pipeline only requires a feed forward through metanetwork and standard finetuning, which is simple,
 341 general and effective. Once we have a metanetwork, we can prune as many networks as we want.
 342 All pruning models are completely different from meta-training data models. This demonstrates our
 343 metanetwork naturally has great transferability and no prior work has done something like this before.
 344 See Appendix A for more comparisons between our work and prior ones (ideas, costs etc.).

345 5.2 CLASSICAL CNN PRUNING TASKS

347 We carry out our experiments on three most classical, popular, and representative image recognition
 348 tasks, including pruning ResNet56 (He et al., 2016) on CIFAR10 (Krizhevsky & Hinton, 2009),
 349 VGG19 (Simonyan & Zisserman, 2015) on CIFAR100 (Krizhevsky & Hinton, 2009) and ResNet50
 350 (He et al., 2016) on ImageNet (Deng et al., 2009). See appendix D.1 for more general setups.

352 Our method achieves outstanding results on all 3 tasks and is better than almost all prior works
 353 (Table 1). See full results compared with prior works in Table 8(ResNet56 on CIFAR10), Ta-
 354 ble 11(VGG19 on CIFAR100), Table 14(ResNet50 on ImageNet). See Appendix D.2 D.3 D.4 for
 355 implementation details on each tasks.

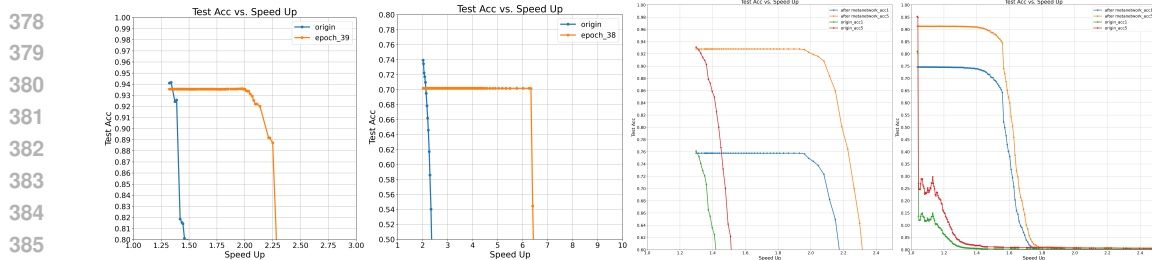
356 Table 1: **Results for 3 classical CNN pruning tasks** including pruning (1) ResNet56 on CIFAR10,
 357 (2) VGG19 on CIFAR100 (3) ResNet50 on ImageNet. For full results compared with prior works,
 358 see (1) Table 8, (2) Table 11, (3) Table 14.

359 Task	360 Base Top-1(Top-5)	361 Pruned Top-1(Δ)	362 Pruned Top-5(Δ)	363 Pruned FLOPs
(1)	93.51%	93.64%(+0.13%)	—	65.6%
(2)	73.65%	69.75%(-3.90%)	—	88.83%
(3)	76.14%(93.11%)	76.13%(-0.01%)	92.78%(-0.33%)	57.2%

364 5.3 ABLATION STUDY OF GENERAL BEHAVIORAL TENDENCIES

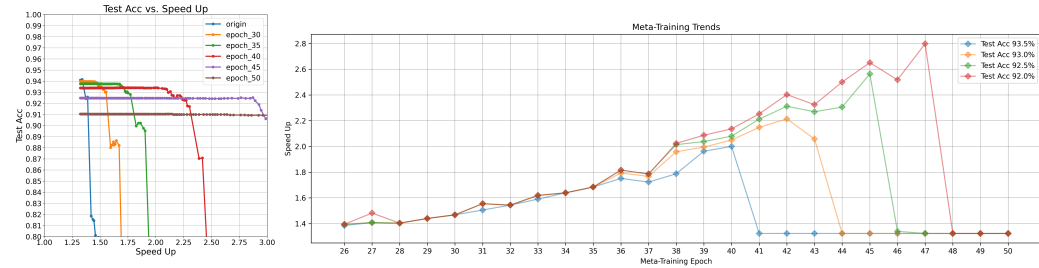
367 **How metanetwork works:** We visualized the "Acc vs. Speed Up" curve of both origin network
 368 and network after feedforward through metanetwork and finetuning (Figure 5). They show that as
 369 the pruning speed up increases, the accuracy drops at a significantly slower rate after applying the
 370 metanetwork and finetuning.

371 **Trade-off between accuracy and speed up:** During meta-training: as the number of training epochs
 372 increases, the metanetwork's ability to make the network easier to prune becomes stronger. However,
 373 its ability to maintain the accuracy becomes weaker. As shown in Figure 6a, with more training
 374 epochs, the "Acc VS. Speed Up" curve shifts downward, and the flat portion of the curve becomes
 375 longer. **This characteristic allows us to adaptively meet different pruning requirements.** If a
 376 higher level of pruning is desired and a moderate drop in accuracy is acceptable, a metanetwork
 377 trained for more epochs would be preferable. Conversely, if preserving accuracy is more important, a
 378 metanetwork trained for fewer epochs would be a better choice (Figure 6b).



(a) ResNet56 on CIFAR10 (b) VGG19 on CIFAR100 (c) ResNet50 on ImageNet (d) ViT on ImageNet

Figure 5: Metanetwork changes hard to prune network into easy to prune network.



(a) Acc VS. Speed Up curves of metanetworks from different meta-training epochs, (b) Feed network through metanetworks from different meta-training epochs, finetuning, then prune it progressively to find the maximum speed up that can maintain the accuracy above a certain threshold.

Figure 6: Trends in meta-training. (ResNet56 on CIFAR10 as example)

Finetuning after Metanetwork. See appendix E.1 for how number of finetuning epochs after metanetwork influence the pruning results.

5.4 ABLATION STUDY OF STATISTICS

We compare the statistics between the origin network and the network after metanetwork(finetuning) to find out how metanetwork transforms the network to make it easier to prune. We mainly visualize the l_2 norm and taylor sensitivity distribution of each layer in Figure 7. Taylor sensitivity here is defined as $w \cdot \Delta L$, it estimates how much the loss will increase if we mask this weight to zero. The larger taylor sensitivity, the more important the weight is and we are unlikely to prune it. More visualization of other statistics are in Appendix H

6 EXPERIMENTS ON TRANSFERABILITY AND FLEXIBILITY

6.1 FLEXIBLE PRUNING CRITERION

Pruning criterion of our method is highly flexible. We build a series of reasonable pruning criterion (Appendix B.2). At first, we directly use MEAN REDUCE, MAX NORMALIZE, $\alpha = 4$ as default, because this is the same as *group norm* in Fang et al. (2023). Later, we keep everything else the same, and try many different criteria, and find they all works well (Table 2). This demonstrates that our framework is robust and has many flexibilities.

6.2 UNSTRUCTURED PRUNING & N:M SPARSITY PRUNING

Most of our experiments are conducted using structured pruning as default. Here we conduct unstructured pruning and N:M sparsity pruning to demonstrate that our methods can be use in all kinds of pruning. We don't use FLOPs to measure the pruning results because unstructured pruning reduces no FLOPs and needs specialized algorithm to accelerate, so we measure the number of parameters instead. See results in Table 3

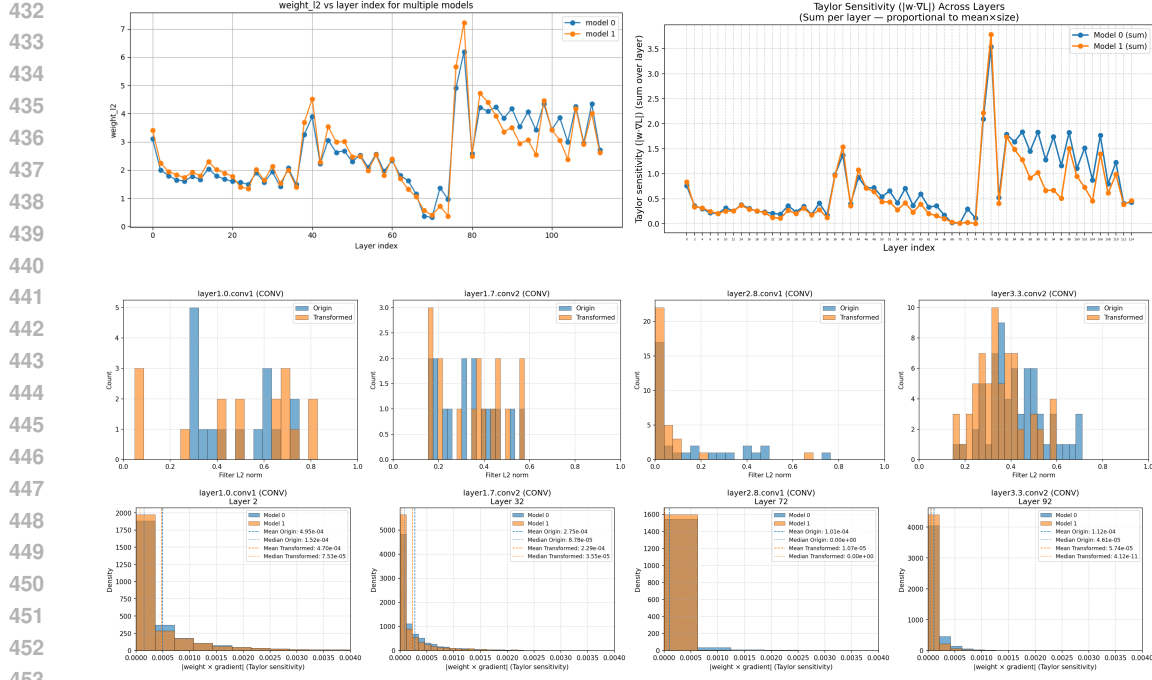


Figure 7: **Statistics:** We compare the statistics of the origin network (orange) and the network after metanetwork and finetuning (blue) when pruning ResNet56 on CIFAR10. The first row is layerwise mean l_2 norm and taylor sensitivity. Then we randomly select several layers and visualize their l_2 norm distribution in row 2 and taylor sensitivity distribution in row 3. **Observation:** Row 1 shows both norm and sensitivity drops on average, especially in the latter part of network where contains a large amount of redundancy and can be substantially pruned. Row 2 shows l_2 norm distribution has been greatly changed. Large norms still exist but more norms tend to be very small. Row 3 shows more parameters become less important under taylor sensitivity.

Table 2: **Flexible pruning criterion:** Pruning ResNet56 on CIFAR10, all experiments use the same origin network with Test Acc 93.51%, all criteria use MEAN REDUCE. We tried different values of Alpha and different ways of NORMALIZE, they all work well. Even in the Naive situation, where we use no NORMALIZE and no shrinkage strength (Alpha is 0), the results remain robust.

	NORMALIZE	alpha	Pruned Acc	Pruned FLOPs	Speed Up
Default	MAX	4	93.64%	65.64%	2.91
Alpha	MAX	0	93.37%	65.75%	2.92
	MAX	2	92.87%	68.15%	3.14
	MAX	6	93.36%	65.75%	2.92
NORMALIZE	MEAN	4	93.42%	65.52%	2.90
	NONE	4	93.08%	65.64%	2.91
Naive	NONE	0	93.04%	65.75%	2.92

Table 3: **Unstructured & N:M sparsity pruning:** Pruning ResNet56 on CIFAR10, meta-train and prune directly with the classical l_1 norm. From the results we can see (1) our framework also works great on unstructured pruning. (2) Unstructured pruning outperforms structured pruning because it is more flexible.

Methods	Pruned Acc	Left Params	Methods	Pruned Acc	Left Params
Unstructured	93.95%	50.25%	Structured(2.9x)	93.49%	42.96%
	94.14%	20.40%		94.02%	75.14%
	93.43%	15.42%		93.97%	50.27%
	92.96%	10.45%		93.13%	25.41%

486 6.3 TRANSFER BETWEEN DATASETS AND ARCHITECTURES
487488 Section 4.4 mentioned that our metanetwork has natural transferability. Following experiments
489 demonstrate that our metanetwork can transfer between similar datasets and network architectures.
490 More relative experiments are in Appendix F.3 F.4491 **Transfer between datasets:** 3 datasets, CIFAR10 (Krizhevsky & Hinton, 2009), CI-
492 FAR100 (Krizhevsky & Hinton, 2009) and SVHN (Goodfellow et al., 2014) are used. We train
493 metanetwork and the to be pruned network on each of them, traverse through every possible combi-
494 nation, and use the metanetwork to prune the network. Results (Table 4) show that out metanetwork can
495 transfer between similar datasets. See Appendix F.1 for full details **Transfer between architectures:**
496497 Table 4: **Transfer between datasets:** All networks’ architecture is ResNet56. Columns represent the
498 training datasets for the metanetwork, and rows represent the training datasets for the to be pruned
499 network. “None” indicates using no metanetwork. Results with metanetwork is obviously better than
500 no metanetwork (The only exception is when training datasets for the to be pruned network is SVHN,
501 and we guess this is because the dataset SVHN itself is too easy).

Dataset\Metanetwork	CIFAR10	CIFAR100	SVHN	None
CIFAR10	93.35	92.47	92.87	91.28
CIFAR100	69.97	70.16	69.25	68.91
SVHN	96.79	96.50	96.86	96.78

502 2 architectures, ResNet56 and ResNet110 (He et al., 2016) are used. We train metanetwork and the
503 to be pruned network on each of them, traverse through every possible combination, and use the
504 metanetwork to prune the network. Results (Table 5) show that our metanetwork can transfer between
505 similar datasets. See Appendix F.2 for full details **Possible Future Use:** For large-scale networks,
506507 Table 5: **Transfer between architectures.** All training dataset is CIFAR10. Columns represent the
508 architectures used for training the metanetwork, and rows represent the architectures of the to be
509 pruned network. “None” indicates using no metanetwork. All results with metanetwork is obviously
510 better than no metanetwork.
511

Architecture\Metanetwork	ResNet56	ResNet110	None
ResNet56	93.40	92.81	92.08
ResNet110	93.04	93.38	92.40

512 the metanetwork can be pretrained on smaller architectures of similar design. And when the original
513 training dataset is unavailable or excessively large, a related dataset may be used for pretraining. This
514 transferability substantially enhances the practicality of the framework.
515524 7 EXPERIMENTS ON TRANSFORMERS
525526 As mentioned in section 4.4, our framework is theoretically applicable to almost all types of networks
527 with all kinds of pruning. Here we expand our implementations to another widely used architecture-
528 transformer (Vaswani et al., 2017). More specifically, we pruned the vision transformer (ViT) from
529 Dosovitskiy et al. (2021) that is trained on ImageNet. See Appendix G for full experiments, including
530 how we convert transformer into graph and conduct further meta-training and pruning.
531532 8 CONCLUSION
533534 We propose an entirely new meta-learning framework for network pruning. For a pruning criterion,
535 we use a metanetwork to change a hard to prune network into another easy to prune network for
536 better pruning. This is a general framework that can be theoretically applied to almost all types of
537 networks with all kinds of pruning. We present practical implementations of our framework and
538 achieve outstanding results. Further analysis and experiments show that our framework has natural
539 generality, flexibility, and transferability.

540 **9 REPRODUCIBILITY STATEMENT**
541542 Our code is available at <https://anonymous.4open.science/r/MetaPruning> together
543 with all the guides to reproduce our experiments.
544545 **REFERENCES**
546547 Tianyi Chen, Luming Liang, Tianyu Ding, Zhihui Zhu, and Ilya Zharkov. Otov2: Automatic, generic,
548 user-friendly. In *The Eleventh International Conference on Learning Representations, ICLR 2023,*
549 *Kigali, Rwanda, May 1-5, 2023*. OpenReview.net, 2023. URL <https://openreview.net/forum?id=7ynoX1ojPMt>.
550551 Hongrong Cheng, Miao Zhang, and Javen Qinfeng Shi. A survey on deep neural network pruning:
552 Taxonomy, comparison, analysis, and recommendations. *IEEE Trans. Pattern Anal. Mach. Intell.*,
553 46(12):10558–10578, 2024. doi: 10.1109/TPAMI.2024.3447085. URL <https://doi.org/10.1109/TPAMI.2024.3447085>.
554555 Gabriele Corso, Luca Cavalleri, Dominique Beaini, Pietro Liò, and Petar Velickovic. Principal neighbourhood aggregation for graph nets. In Hugo Larochelle, Marc’Aurelio Ranzato, Raia Hadsell, Maria-Florina Balcan, and Hsuan-Tien Lin (eds.), *Advances in Neural Information Processing Systems 33: Annual Conference on Neural Information Processing Systems 2020, NeurIPS 2020, December 6-12, 2020, virtual*, 2020. URL <https://proceedings.neurips.cc/paper/2020/hash/99cad265a1768cc2dd013f0e740300ae-Abstract.html>.
556557 Jia Deng, Wei Dong, Richard Socher, Li-Jia Li, Kai Li, and Li Fei-Fei. Imagenet: A large-scale
558 hierarchical image database. In *2009 IEEE Computer Society Conference on Computer Vision and*
559 *Pattern Recognition (CVPR 2009), 20-25 June 2009, Miami, Florida, USA*, pp. 248–255. IEEE
560 Computer Society, 2009. doi: 10.1109/CVPR.2009.5206848. URL <https://doi.org/10.1109/CVPR.2009.5206848>.
561562 Lucio M. Dery, Steven Kolawole, Jean-François Kagey, Virginia Smith, Graham Neubig, and Ameet
563 Talwalkar. Everybody prune now: Structured pruning of llms with only forward passes. *CoRR*,
564 abs/2402.05406, 2024. doi: 10.48550/ARXIV.2402.05406. URL <https://doi.org/10.48550/arXiv.2402.05406>.
565566 Xiaohan Ding, Guiguang Ding, Jungong Han, and Sheng Tang. Auto-balanced filter pruning for
567 efficient convolutional neural networks. In Sheila A. McIlraith and Kilian Q. Weinberger (eds.),
568 *Proceedings of the Thirty-Second AAAI Conference on Artificial Intelligence, (AAAI-18), the*
569 *30th innovative Applications of Artificial Intelligence (IAAI-18), and the 8th AAAI Symposium*
570 *on Educational Advances in Artificial Intelligence (EAAI-18), New Orleans, Louisiana, USA,*
571 *February 2-7, 2018*, pp. 6797–6804. AAAI Press, 2018. doi: 10.1609/AAAI.V32I1.12262. URL
572 <https://doi.org/10.1609/aaai.v32i1.12262>.
573574 Xiaohan Ding, Guiguang Ding, Yuchen Guo, and Jungong Han. Centripetal SGD for pruning very
575 deep convolutional networks with complicated structure. In *IEEE Conference on Computer*
576 *Vision and Pattern Recognition, CVPR 2019, Long Beach, CA, USA, June 16-20, 2019*, pp.
577 4943–4953. Computer Vision Foundation / IEEE, 2019. doi: 10.1109/CVPR.2019.00508.
578 URL http://openaccess.thecvf.com/content_CVPR_2019/html/Ding_Centripetal_SGD_for_Pruning_Very_Deep_Convolutional_Networks_With_Complicated_CVPR_2019_paper.html.
579580 Xiaohan Ding, Tianxiang Hao, Jianchao Tan, Ji Liu, Jungong Han, Yuchen Guo, and Guiguang
581 Ding. Resrep: Lossless CNN pruning via decoupling remembering and forgetting. In *2021*
582 *IEEE/CVF International Conference on Computer Vision, ICCV 2021, Montreal, QC, Canada,*
583 *October 10-17, 2021*, pp. 4490–4500. IEEE, 2021. doi: 10.1109/ICCV48922.2021.00447. URL
584 <https://doi.org/10.1109/ICCV48922.2021.00447>.
585586 Alexey Dosovitskiy, Lucas Beyer, Alexander Kolesnikov, Dirk Weissenborn, Xiaohua Zhai, Thomas
587 Unterthiner, Mostafa Dehghani, Matthias Minderer, Georg Heigold, Sylvain Gelly, Jakob Uszkoreit,
588 and Neil Houlsby. An image is worth 16x16 words: Transformers for image recognition at scale.
589 In *9th International Conference on Learning Representations, ICLR 2021, Virtual Event, Austria*,
590

594 May 3-7, 2021. OpenReview.net, 2021. URL <https://openreview.net/forum?id=YicbFdNTTy>.

595

596

597 Gongfan Fang, Xinyin Ma, Mingli Song, Michael Bi Mi, and Xinchao Wang. Depgraph: Towards
598 any structural pruning. In *IEEE/CVF Conference on Computer Vision and Pattern Recognition,
599 CVPR 2023, Vancouver, BC, Canada, June 17-24, 2023*, pp. 16091–16101. IEEE, 2023. doi: 10.
600 1109/CVPR52729.2023.01544. URL <https://doi.org/10.1109/CVPR52729.2023.01544>.

601

602 Jonathan Frankle and Michael Carbin. The lottery ticket hypothesis: Finding sparse, trainable
603 neural networks. In *7th International Conference on Learning Representations, ICLR 2019, New
604 Orleans, LA, USA, May 6-9, 2019*. OpenReview.net, 2019. URL <https://openreview.net/forum?id=rJl-b3RcF7>.

605

606

607 Shangqian Gao, Feihu Huang, Jian Pei, and Heng Huang. Discrete model compression with
608 resource constraint for deep neural networks. In *2020 IEEE/CVF Conference on Computer
609 Vision and Pattern Recognition, CVPR 2020, Seattle, WA, USA, June 13-19, 2020*, pp. 1896–
610 1905. Computer Vision Foundation / IEEE, 2020. doi: 10.1109/CVPR42600.2020.00197.
611 URL https://openaccess.thecvf.com/content_CVPR_2020/html/Gao_Discrete_Model_Compression_With_Resource_Constraint_for_Deep_Neural_Networks_CVPR_2020_paper.html.

612

613

614 Justin Gilmer, Samuel S. Schoenholz, Patrick F. Riley, Oriol Vinyals, and George E. Dahl. Neural
615 message passing for quantum chemistry. In Doina Precup and Yee Whye Teh (eds.), *Proceedings
616 of the 34th International Conference on Machine Learning, ICML 2017, Sydney, NSW, Australia,
617 6-11 August 2017*, volume 70 of *Proceedings of Machine Learning Research*, pp. 1263–1272.
618 PMLR, 2017. URL <http://proceedings.mlr.press/v70/gilmer17a.html>.

619

620 Ross B. Girshick, Jeff Donahue, Trevor Darrell, and Jitendra Malik. Rich feature hierarchies for
621 accurate object detection and semantic segmentation. In *2014 IEEE Conference on Computer
622 Vision and Pattern Recognition, CVPR 2014, Columbus, OH, USA, June 23-28, 2014*, pp. 580–587.
623 IEEE Computer Society, 2014. doi: 10.1109/CVPR.2014.81. URL <https://doi.org/10.1109/CVPR.2014.81>.

624

625 Charles Godfrey, Davis Brown, Tegan Emerson, and Henry Kvinge. On the symmetries
626 of deep learning models and their internal representations. In Sanmi Koyejo, S. Mo-
627 hammed, A. Agarwal, Danielle Belgrave, K. Cho, and A. Oh (eds.), *Advances in Neural
628 Information Processing Systems 35: Annual Conference on Neural Information Process-
629 ing Systems 2022, NeurIPS 2022, New Orleans, LA, USA, November 28 - December 9,
630 2022*, 2022. URL http://papers.nips.cc/paper_files/paper/2022/hash/4df3510ad02a86d69dc32388d91606f8-Abstract-Conference.html.

631

632 Ian J. Goodfellow, Yaroslav Bulatov, Julian Ibarz, Sacha Arnoud, and Vinay D. Shet. Multi-digit
633 number recognition from street view imagery using deep convolutional neural networks. In
634 Yoshua Bengio and Yann LeCun (eds.), *2nd International Conference on Learning Representations,
635 ICLR 2014, Banff, AB, Canada, April 14-16, 2014, Conference Track Proceedings*, 2014. URL
636 <http://arxiv.org/abs/1312.6082>.

637

638 Ariel Gordon, Elad Eban, Ofir Nachum, Bo Chen, Hao Wu, Tien-Ju Yang, and Edward Choi.
639 Morphnet: Fast & simple resource-constrained structure learning of deep networks. In *2018 IEEE
640 Conference on Computer Vision and Pattern Recognition, CVPR 2018, Salt Lake City, UT, USA,
641 June 18-22, 2018*, pp. 1586–1595. Computer Vision Foundation / IEEE Computer Society, 2018.
642 doi: 10.1109/CVPR.2018.00171. URL https://openaccess.thecvf.com/content_cvpr_2018/html/Gordon_MorphNet_Fast__CVPR_2018_paper.html.

643

644 Song Han, Huizi Mao, and William J. Dally. Deep compression: Compressing deep neural network
645 with pruning, trained quantization and huffman coding. In Yoshua Bengio and Yann LeCun (eds.),
646 *4th International Conference on Learning Representations, ICLR 2016, San Juan, Puerto Rico,
647 May 2-4, 2016, Conference Track Proceedings*, 2016. URL <http://arxiv.org/abs/1510.00149>.

648 Kaiming He, Xiangyu Zhang, Shaoqing Ren, and Jian Sun. Deep residual learning for image
 649 recognition. In *2016 IEEE Conference on Computer Vision and Pattern Recognition, CVPR*
 650 *2016, Las Vegas, NV, USA, June 27-30, 2016*, pp. 770–778. IEEE Computer Society, 2016. doi:
 651 10.1109/CVPR.2016.90. URL <https://doi.org/10.1109/CVPR.2016.90>.

652 Yang He and Lingao Xiao. Structured pruning for deep convolutional neural networks: A survey. *IEEE*
 653 *Trans. Pattern Anal. Mach. Intell.*, 46(5):2900–2919, 2024. doi: 10.1109/TPAMI.2023.3334614.
 654 URL <https://doi.org/10.1109/TPAMI.2023.3334614>.

655 Yang He, Guoliang Kang, Xuanyi Dong, Yanwei Fu, and Yi Yang. Soft filter pruning for accelerating
 656 deep convolutional neural networks. In Jérôme Lang (ed.), *Proceedings of the Twenty-Seventh*
 657 *International Joint Conference on Artificial Intelligence, IJCAI 2018, July 13-19, 2018, Stockholm,*
 658 *Sweden*, pp. 2234–2240. ijcai.org, 2018a. doi: 10.24963/IJCAI.2018/309. URL <https://doi.org/10.24963/ijcai.2018/309>.

659 Yang He, Ping Liu, Ziwei Wang, Zhilan Hu, and Yi Yang. Filter pruning via geometric median
 660 for deep convolutional neural networks acceleration. In *IEEE Conference on Computer*
 661 *Vision and Pattern Recognition, CVPR 2019, Long Beach, CA, USA, June 16-20, 2019*, pp.
 662 4340–4349. Computer Vision Foundation / IEEE, 2019a. doi: 10.1109/CVPR.2019.00447. URL
 663 http://openaccess.thecvf.com/content_CVPR_2019/html/He_Filter_Pruning_via_Geometric_Median_for_Deep_Convolutional_Neural_Networks_CVPR_2019_paper.html.

664 Yang He, Ping Liu, Ziwei Wang, Zhilan Hu, and Yi Yang. Filter pruning via geometric median
 665 for deep convolutional neural networks acceleration. In *IEEE Conference on Computer*
 666 *Vision and Pattern Recognition, CVPR 2019, Long Beach, CA, USA, June 16-20, 2019*, pp.
 667 4340–4349. Computer Vision Foundation / IEEE, 2019b. doi: 10.1109/CVPR.2019.00447. URL
 668 http://openaccess.thecvf.com/content_CVPR_2019/html/He_Filter_Pruning_via_Geometric_Median_for_Deep_Convolutional_Neural_Networks_CVPR_2019_paper.html.

669 Yang He, Yuhang Ding, Ping Liu, Linchao Zhu, Hanwang Zhang, and Yi Yang. Learning filter prun-
 670 ing criteria for deep convolutional neural networks acceleration. In *2020 IEEE/CVF Conference*
 671 *on Computer Vision and Pattern Recognition, CVPR 2020, Seattle, WA, USA, June 13-19, 2020*, pp.
 672 2006–2015. Computer Vision Foundation / IEEE, 2020. doi: 10.1109/CVPR42600.2020.00208.
 673 URL https://openaccess.thecvf.com/content_CVPR_2020/html/He_Learning_Filter_Pruning_Criteria_for_Deep_Convolutional_Neural_Networks_Acceleration_CVPR_2020_paper.html.

674 Yihui He, Xiangyu Zhang, and Jian Sun. Channel pruning for accelerating very deep neural networks.
 675 In *IEEE International Conference on Computer Vision, ICCV 2017, Venice, Italy, October 22-29, 2017*, pp. 1398–1406. IEEE Computer Society, 2017. doi: 10.1109/ICCV.2017.155. URL
 676 <https://doi.org/10.1109/ICCV.2017.155>.

677 Yihui He, Ji Lin, Zhijian Liu, Hanrui Wang, Li-Jia Li, and Song Han. AMC: automl for model
 678 compression and acceleration on mobile devices. In Vittorio Ferrari, Martial Hebert, Cristian
 679 Sminchisescu, and Yair Weiss (eds.), *Computer Vision - ECCV 2018 - 15th European Conference,*
 680 *Munich, Germany, September 8-14, 2018, Proceedings, Part VII*, volume 11211 of *Lecture Notes*
 681 *in Computer Science*, pp. 815–832. Springer, 2018b. doi: 10.1007/978-3-030-01234-2_48. URL
 682 https://doi.org/10.1007/978-3-030-01234-2_48.

683 Timothy M. Hospedales, Antreas Antoniou, Paul Micaelli, and Amos J. Storkey. Meta-learning
 684 in neural networks: A survey. *IEEE Trans. Pattern Anal. Mach. Intell.*, 44(9):5149–5169, 2022.
 685 doi: 10.1109/TPAMI.2021.3079209. URL <https://doi.org/10.1109/TPAMI.2021.3079209>.

686 Zehao Huang and Naiyan Wang. Data-driven sparse structure selection for deep neural networks.
 687 In Vittorio Ferrari, Martial Hebert, Cristian Sminchisescu, and Yair Weiss (eds.), *Computer*
 688 *Vision - ECCV 2018 - 15th European Conference, Munich, Germany, September 8-14, 2018,*
 689 *Proceedings, Part XVI*, volume 11220 of *Lecture Notes in Computer Science*, pp. 317–334.
 690 Springer, 2018. doi: 10.1007/978-3-030-01270-0_19. URL https://doi.org/10.1007/978-3-030-01270-0_19.

702 Sergey Ioffe and Christian Szegedy. Batch normalization: Accelerating deep network training by
 703 reducing internal covariate shift. In Francis R. Bach and David M. Blei (eds.), *Proceedings of the*
 704 *32nd International Conference on Machine Learning, ICML 2015, Lille, France, 6-11 July 2015*,
 705 volume 37 of *JMLR Workshop and Conference Proceedings*, pp. 448–456. JMLR.org, 2015. URL
 706 <http://proceedings.mlr.press/v37/ioffe15.html>.

707 Ioannis Kalogeropoulos, Giorgos Bouritsas, and Yannis Panagakis. Scale equivariant
 708 graph metanetworks. In Amir Globersons, Lester Mackey, Danielle Belgrave, Angela
 709 Fan, Ulrich Paquet, Jakub M. Tomczak, and Cheng Zhang (eds.), *Advances in Neu-*
 710 *ral Information Processing Systems 38: Annual Conference on Neural Information Pro-*
 711 *cessing Systems 2024, NeurIPS 2024, Vancouver, BC, Canada, December 10 - 15,*
 712 *2024*, 2024. URL http://papers.nips.cc/paper_files/paper/2024/hash/c13d5a10028586fdc15ee7da97b7563f-Abstract-Conference.html.

713 Minsoo Kang and Bohyung Han. Operation-aware soft channel pruning using differentiable masks.
 714 In *Proceedings of the 37th International Conference on Machine Learning, ICML 2020, 13-18 July*
 715 *2020, Virtual Event*, volume 119 of *Proceedings of Machine Learning Research*, pp. 5122–5131.
 716 PMLR, 2020. URL <http://proceedings.mlr.press/v119/kang20a.html>.

717 Thomas N. Kipf and Max Welling. Semi-supervised classification with graph convolutional networks.
 718 In *5th International Conference on Learning Representations, ICLR 2017, Toulon, France, April 24-*
 719 *26, 2017, Conference Track Proceedings*. OpenReview.net, 2017. URL <https://openreview.net/forum?id=SJU4ayYgl>.

720 Miltiadis Kofinas, Boris Knyazev, Yan Zhang, Yunlu Chen, Gertjan J. Burghouts, Efstratios Gavves,
 721 Cees G. M. Snoek, and David W. Zhang. Graph neural networks for learning equivariant rep-
 722 resentations of neural networks. In *The Twelfth International Conference on Learning Rep-*
 723 *resentations, ICLR 2024, Vienna, Austria, May 7-11, 2024*. OpenReview.net, 2024. URL
 724 <https://openreview.net/forum?id=oO6FsMyDBt>.

725 Alex Krizhevsky and Geoffrey Hinton. Learning multiple layers of features from tiny images.
 726 Technical Report 0, University of Toronto, Toronto, Ontario, 2009. URL <https://www.cs.toronto.edu/~kriz/learning-features-2009-TR.pdf>.

727 Yann LeCun, John S. Denker, and Sara A. Solla. Optimal brain damage. In David S. Touretzky
 728 (ed.), *Advances in Neural Information Processing Systems 2, [NIPS Conference, Denver, Colorado,*
 729 *USA, November 27-30, 1989]*, pp. 598–605. Morgan Kaufmann, 1989. URL <http://papers.nips.cc/paper/250-optimal-brain-damage>.

730 Yann LeCun, Yoshua Bengio, and Geoffrey E. Hinton. Deep learning. *Nat.*, 521(7553):436–444,
 731 2015. doi: 10.1038/NATURE14539. URL <https://doi.org/10.1038/nature14539>.

732 Namhoon Lee, Thalaiyasingam Ajanthan, and Philip H. S. Torr. Snip: single-shot network pruning
 733 based on connection sensitivity. In *7th International Conference on Learning Representations,*
 734 *ICLR 2019, New Orleans, LA, USA, May 6-9, 2019*. OpenReview.net, 2019. URL <https://openreview.net/forum?id=B1VZqjAcYX>.

735 Hao Li, Asim Kadav, Igor Durdanovic, Hanan Samet, and Hans Peter Graf. Pruning filters for
 736 efficient convnets. In *5th International Conference on Learning Representations, ICLR 2017,*
 737 *Toulon, France, April 24-26, 2017, Conference Track Proceedings*. OpenReview.net, 2017a. URL
 738 <https://openreview.net/forum?id=rJqFGTs1g>.

739 Hao Li, Asim Kadav, Igor Durdanovic, Hanan Samet, and Hans Peter Graf. Pruning filters for
 740 efficient convnets. In *5th International Conference on Learning Representations, ICLR 2017,*
 741 *Toulon, France, April 24-26, 2017, Conference Track Proceedings*. OpenReview.net, 2017b. URL
 742 <https://openreview.net/forum?id=rJqFGTs1g>.

743 Yawei Li, Shuhang Gu, Kai Zhang, Luc Van Gool, and Radu Timofte. DHP: differentiable meta
 744 pruning via hypernetworks. In Andrea Vedaldi, Horst Bischof, Thomas Brox, and Jan-Michael
 745 Frahm (eds.), *Computer Vision - ECCV 2020 - 16th European Conference, Glasgow, UK, August*
 746 *23-28, 2020, Proceedings, Part VIII*, volume 12353 of *Lecture Notes in Computer Science*, pp.
 747 608–624. Springer, 2020. doi: 10.1007/978-3-030-58598-3_36. URL https://doi.org/10.1007/978-3-030-58598-3_36.

756 Yawei Li, Kamil Adamczewski, Wen Li, Shuhang Gu, Radu Timofte, and Luc Van Gool. Revisiting
 757 random channel pruning for neural network compression. In *IEEE/CVF Conference on Computer*
 758 *Vision and Pattern Recognition, CVPR 2022, New Orleans, LA, USA, June 18-24, 2022*, pp.
 759 191–201. IEEE, 2022. doi: 10.1109/CVPR52688.2022.00029. URL <https://doi.org/10.1109/CVPR52688.2022.00029>.

760

761 Yunqiang Li, Jan C. van Gemert, Torsten Hoefer, Bert Moons, Evangelos Eleftheriou, and Bram-
 762 Ernst Verhoef. Differentiable transportation pruning. In *IEEE/CVF International Conference on*
 763 *Computer Vision, ICCV 2023, Paris, France, October 1-6, 2023*, pp. 16911–16921. IEEE, 2023.
 764 doi: 10.1109/ICCV51070.2023.01555. URL <https://doi.org/10.1109/ICCV51070.2023.01555>.

765

766

767 Derek Lim, Haggai Maron, Marc T. Law, Jonathan Lorraine, and James Lucas. Graph metanetworks
 768 for processing diverse neural architectures. In *The Twelfth International Conference on Learning*
 769 *Representations, ICLR 2024, Vienna, Austria, May 7-11, 2024*. OpenReview.net, 2024. URL
 770 <https://openreview.net/forum?id=ijk5hyxs0n>.

771

772 Mingbao Lin, Rongrong Ji, Yan Wang, Yichen Zhang, Baochang Zhang, Yonghong Tian, and Ling
 773 Shao. Hrank: Filter pruning using high-rank feature map. In *2020 IEEE/CVF Conference on Com-*
 774 *puter Vision and Pattern Recognition, CVPR 2020, Seattle, WA, USA, June 13-19, 2020*, pp. 1526–
 775 1535. Computer Vision Foundation / IEEE, 2020a. doi: 10.1109/CVPR42600.2020.00160. URL
 776 https://openaccess.thecvf.com/content_CVPR_2020/html/Lin_HRank_Filter_Pruning_Using_High-Rank_Feature_Map_CVPR_2020_paper.html.

777

778 Mingbao Lin, Rongrong Ji, Yuxin Zhang, Baochang Zhang, Yongjian Wu, and Yonghong Tian.
 779 Channel pruning via automatic structure search. In Christian Bessiere (ed.), *Proceedings of*
 780 *the Twenty-Ninth International Joint Conference on Artificial Intelligence, IJCAI 2020*, pp. 673–
 781 679. ijcai.org, 2020b. doi: 10.24963/IJCAI.2020/94. URL <https://doi.org/10.24963/ijcai.2020/94>.

782

783 Shaohui Lin, Rongrong Ji, Chenqian Yan, Baochang Zhang, Liujuan Cao, Qixiang Ye, Feiyue Huang,
 784 and David S. Doermann. Towards optimal structured CNN pruning via generative adversarial
 785 learning. In *IEEE Conference on Computer Vision and Pattern Recognition, CVPR 2019, Long*
 786 *Beach, CA, USA, June 16-20, 2019*, pp. 2790–2799. Computer Vision Foundation / IEEE, 2019.
 787 doi: 10.1109/CVPR.2019.00290. URL http://openaccess.thecvf.com/content_CVPR_2019/html/Lin_Towards_Optimal_Structured_CNN_Pruning_via_Generative_Adversarial_Learning_CVPR_2019_paper.html.

788

789

790 Shaohui Lin, Rongrong Ji, Yuchao Li, Cheng Deng, and Xuelong Li. Toward compact convnets via
 791 structure-sparsity regularized filter pruning. *IEEE Trans. Neural Networks Learn. Syst.*, 31(2):
 792 574–588, 2020c. doi: 10.1109/TNNLS.2019.2906563. URL <https://doi.org/10.1109/TNNLS.2019.2906563>.

793

794

795 Zechun Liu, Haoyuan Mu, Xiangyu Zhang, Zichao Guo, Xin Yang, Kwang-Ting Cheng, and Jian
 796 Sun. Metapruning: Meta learning for automatic neural network channel pruning. In *2019*
 797 *IEEE/CVF International Conference on Computer Vision, ICCV 2019, Seoul, Korea (South),*
 798 *October 27 - November 2, 2019*, pp. 3295–3304. IEEE, 2019. doi: 10.1109/ICCV.2019.00339.
 799 URL <https://doi.org/10.1109/ICCV.2019.00339>.

800

801 Xinyin Ma, Gongfan Fang, and Xinchao Wang. Llm-pruner: On the structural pruning of large
 802 language models. In Alice Oh, Tristan Naumann, Amir Globerson, Kate Saenko, Moritz Hardt, and
 803 Sergey Levine (eds.), *Advances in Neural Information Processing Systems 36: Annual Conference*
 804 *on Neural Information Processing Systems 2023, NeurIPS 2023, New Orleans, LA, USA, December*
 805 *10 - 16, 2023*, 2023. URL http://papers.nips.cc/paper_files/paper/2023/hash/44956951349095f74492a5471128a7e0-Abstract-Conference.html.

806

807 Haggai Maron, Heli Ben-Hamu, Nadav Shamir, and Yaron Lipman. Invariant and equivariant graph
 808 networks. In *7th International Conference on Learning Representations, ICLR 2019, New Orleans,*
 809 *LA, USA, May 6-9, 2019*. OpenReview.net, 2019. URL <https://openreview.net/forum?id=Syx72jC9tm>.

810 Pavlo Molchanov, Arun Mallya, Stephen Tyree, Iuri Frosio, and Jan Kautz. Importance estimation for
 811 neural network pruning. In *IEEE Conference on Computer Vision and Pattern Recognition, CVPR*
 812 *2019, Long Beach, CA, USA, June 16-20, 2019*, pp. 11264–11272. Computer Vision Foundation
 813 / IEEE, 2019. doi: 10.1109/CVPR.2019.01152. URL http://openaccess.thecvf.com/content_CVPR_2019/html/Molchanov_Importance_Estimation_for_Neural_Network_Pruning_CVPR_2019_paper.html.

814

815

816 Aviv Navon, Aviv Shamsian, Idan Achituv, Ethan Fetaya, Gal Chechik, and Haggai Maron. Equivariant
 817 architectures for learning in deep weight spaces. In Andreas Krause, Emma Brunskill,
 818 Kyunghyun Cho, Barbara Engelhardt, Sivan Sabato, and Jonathan Scarlett (eds.), *International*
 819 *Conference on Machine Learning, ICML 2023, 23-29 July 2023, Honolulu, Hawaii, USA*, volume
 820 202 of *Proceedings of Machine Learning Research*, pp. 25790–25816. PMLR, 2023. URL
 821 <https://proceedings.mlr.press/v202/navon23a.html>.

822

823 Hanyu Peng, Jiaxiang Wu, Shifeng Chen, and Junzhou Huang. Collaborative channel pruning for
 824 deep networks. In Kamalika Chaudhuri and Ruslan Salakhutdinov (eds.), *Proceedings of the*
 825 *36th International Conference on Machine Learning, ICML 2019, 9-15 June 2019, Long Beach,*
 826 *California, USA*, volume 97 of *Proceedings of Machine Learning Research*, pp. 5113–5122. PMLR,
 827 2019. URL <http://proceedings.mlr.press/v97/peng19c.html>.

828

829 Yongming Rao, Jiwen Lu, Ji Lin, and Jie Zhou. Runtime network routing for efficient image
 830 classification. *IEEE Trans. Pattern Anal. Mach. Intell.*, 41(10):2291–2304, 2019. doi: 10.1109/TPAMI.2018.2878258. URL <https://doi.org/10.1109/TPAMI.2018.2878258>.

831

832 Russell Reed. Pruning algorithms-a survey. *IEEE Trans. Neural Networks*, 4(5):740–747, 1993. doi:
 833 10.1109/72.248452. URL <https://doi.org/10.1109/72.248452>.

834

835 Franco Scarselli, Marco Gori, Ah Chung Tsoi, Markus Hagenbuchner, and Gabriele Monfardini. The
 836 graph neural network model. *IEEE Trans. Neural Networks*, 20(1):61–80, 2009. doi: 10.1109/TNN.2008.2005605. URL <https://doi.org/10.1109/TNN.2008.2005605>.

837

838 Jürgen Schmidhuber. Deep learning in neural networks: An overview. *Neural Networks*, 61:85–
 839 117, 2015. doi: 10.1016/J.NEUNET.2014.09.003. URL <https://doi.org/10.1016/j.neunet.2014.09.003>.

840

841 Karen Simonyan and Andrew Zisserman. Very deep convolutional networks for large-scale image
 842 recognition. In Yoshua Bengio and Yann LeCun (eds.), *3rd International Conference on Learning*
 843 *Representations, ICLR 2015, San Diego, CA, USA, May 7-9, 2015, Conference Track Proceedings*,
 844 2015. URL <http://arxiv.org/abs/1409.1556>.

845

846 Zhuoran Song, Yihong Xu, Zhezhi He, Li Jiang, Naifeng Jing, and Xiaoyao Liang. Cp-vit: Cascade
 847 vision transformer pruning via progressive sparsity prediction, 2022. URL <https://arxiv.org/abs/2203.04570>.

848

849 Mingjie Sun, Zhuang Liu, Anna Bair, and J. Zico Kolter. A simple and effective pruning approach for
 850 large language models. In *The Twelfth International Conference on Learning Representations, ICLR*
 851 *2024, Vienna, Austria, May 7-11, 2024*. OpenReview.net, 2024. URL <https://openreview.net/forum?id=PxoFut3dWW>.

852

853

854 Hoang Tran, Thieu Vo, Tho Huu, An Nguyen The, and Tan Nguyen. Monomial matrix
 855 group equivariant neural functional networks. In Amir Globersons, Lester Mackey, Danielle
 856 Belgrave, Angela Fan, Ulrich Paquet, Jakub M. Tomczak, and Cheng Zhang (eds.), *Advances in Neural*
 857 *Information Processing Systems 38: Annual Conference on Neural Information Processing Systems 2024, NeurIPS 2024, Vancouver, BC, Canada, December 10 - 15,*
 858 *2024, 2024a*. URL http://papers.nips.cc/paper_files/paper/2024/hash/577cd5863ec73be4e6871340be0936ae-Abstract-Conference.html.

859

860

861 Viet-Hoang Tran, Thieu N. Vo, An Nguyen The, Tho Tran Huu, Minh-Khoi Nguyen-Nhat, Thanh
 862 Tran, Duy-Tung Pham, and Tan Minh Nguyen. Equivariant neural functional networks for
 863 transformers. *CoRR*, abs/2410.04209, 2024b. doi: 10.48550/ARXIV.2410.04209. URL <https://doi.org/10.48550/arXiv.2410.04209>.

864 Thomas Unterthiner, Daniel Keysers, Sylvain Gelly, Olivier Bousquet, and Ilya O. Tolstikhin. Predicting neural network accuracy from weights. *CoRR*, abs/2002.11448, 2020. URL <https://arxiv.org/abs/2002.11448>.

865

866

867

868 Ashish Vaswani, Noam Shazeer, Niki Parmar, Jakob Uszkoreit, Llion Jones, Aidan N Gomez,
869 Łukasz Kaiser, and Illia Polosukhin. Attention is all you need. In I. Guyon, U. Von
870 Luxburg, S. Bengio, H. Wallach, R. Fergus, S. Vishwanathan, and R. Garnett (eds.), *Advances in Neural Information Processing Systems*, volume 30. Curran Associates, Inc.,
871 2017. URL https://proceedings.neurips.cc/paper_files/paper/2017/file/3f5ee243547dee91fb053c1c4a845aa-Paper.pdf.

872

873

874 Chaoqi Wang, Roger B. Grosse, Sanja Fidler, and Guodong Zhang. Eigendamage: Structured pruning
875 in the kronecker-factored eigenbasis. In Kamalika Chaudhuri and Ruslan Salakhutdinov (eds.),
876 *Proceedings of the 36th International Conference on Machine Learning, ICML 2019, 9-15 June
877 2019, Long Beach, California, USA*, volume 97 of *Proceedings of Machine Learning Research*,
878 pp. 6566–6575. PMLR, 2019. URL <http://proceedings.mlr.press/v97/wang19g.html>.

879

880 Huan Wang, Can Qin, Yulun Zhang, and Yun Fu. Neural pruning via growing regularization. In *9th
881 International Conference on Learning Representations, ICLR 2021, Virtual Event, Austria, May
882 3-7, 2021*. OpenReview.net, 2021. URL https://openreview.net/forum?id=o966_Is_nPA.

883

884 Huan Wang, Can Qin, Yue Bai, Yulun Zhang, and Yun Fu. Recent advances on neural network
885 pruning at initialization. In Luc De Raedt (ed.), *Proceedings of the Thirty-First International
886 Joint Conference on Artificial Intelligence, IJCAI 2022, Vienna, Austria, 23-29 July 2022*, pp.
887 5638–5645. ijcai.org, 2022. doi: 10.24963/IJCAI.2022/786. URL <https://doi.org/10.24963/ijcai.2022/786>.

888

889 Wei Wen, Chunpeng Wu, Yandan Wang, Yiran Chen, and Hai Li. Learning structured sparsity
890 in deep neural networks. In Daniel D. Lee, Masashi Sugiyama, Ulrike von Luxburg, Isabelle
891 Guyon, and Roman Garnett (eds.), *Advances in Neural Information Processing Systems 29: Annual
892 Conference on Neural Information Processing Systems 2016, December 5-10, 2016, Barcelona,
893 Spain*, pp. 2074–2082, 2016. URL <https://proceedings.neurips.cc/paper/2016/hash/41bfd20a38bb1b0bec75acf0845530a7-Abstract.html>.

894

895

896 Xidong Wu, Shangqian Gao, Zeyu Zhang, Zhenzhen Li, Runxue Bao, Yanfu Zhang, Xiaoqian Wang,
897 and Heng Huang. Auto- train-once: Controller network guided automatic network pruning from
898 scratch. In *IEEE/CVF Conference on Computer Vision and Pattern Recognition, CVPR 2024,
899 Seattle, WA, USA, June 16-22, 2024*, pp. 16163–16173. IEEE, 2024. doi: 10.1109/CVPR52733.
900 2024.01530. URL <https://doi.org/10.1109/CVPR52733.2024.01530>.

901

902 Zonghan Wu, Shirui Pan, Fengwen Chen, Guodong Long, Chengqi Zhang, and Philip S. Yu. A
903 comprehensive survey on graph neural networks. *IEEE Trans. Neural Networks Learn. Syst.*, 32
904 (1):4–24, 2021. doi: 10.1109/TNNLS.2020.2978386. URL <https://doi.org/10.1109/TNNLS.2020.2978386>.

905

906 Mengzhou Xia, Zexuan Zhong, and Danqi Chen. Structured pruning learns compact and accurate
907 models. In Smaranda Muresan, Preslav Nakov, and Aline Villavicencio (eds.), *Proceedings of the
908 60th Annual Meeting of the Association for Computational Linguistics (Volume 1: Long Papers),
909 ACL 2022, Dublin, Ireland, May 22-27, 2022*, pp. 1513–1528. Association for Computational
910 Linguistics, 2022. doi: 10.18653/V1/2022.ACL-LONG.107. URL <https://doi.org/10.18653/v1/2022.acl-long.107>.

911

912 Mengzhou Xia, Tianyu Gao, Zhiyuan Zeng, and Danqi Chen. Sheared llama: Accelerating language
913 model pre-training via structured pruning. In *The Twelfth International Conference on Learning
914 Representations, ICLR 2024, Vienna, Austria, May 7-11, 2024*. OpenReview.net, 2024. URL
915 <https://openreview.net/forum?id=09iOdaeOzp>.

916

917 Mao Ye, Chengyue Gong, Lizhen Nie, Denny Zhou, Adam R. Klivans, and Qiang Liu. Good
918 subnetworks provably exist: Pruning via greedy forward selection. In *Proceedings of the 37th
919 International Conference on Machine Learning, ICML 2020, 13-18 July 2020, Virtual Event*,

918 volume 119 of *Proceedings of Machine Learning Research*, pp. 10820–10830. PMLR, 2020. URL
 919 <http://proceedings.mlr.press/v119/ye20b.html>.

920

921 Zhonghui You, Kun Yan, Jinmian Ye, Meng Ma, and Ping Wang. Gate decorator: Global filter
 922 pruning method for accelerating deep convolutional neural networks. In Hanna M. Wallach, Hugo
 923 Larochelle, Alina Beygelzimer, Florence d’Alché-Buc, Emily B. Fox, and Roman Garnett (eds.),
 924 *Advances in Neural Information Processing Systems 32: Annual Conference on Neural Information
 925 Processing Systems 2019, NeurIPS 2019, December 8-14, 2019, Vancouver, BC, Canada*, pp.
 926 2130–2141, 2019a. URL <https://proceedings.neurips.cc/paper/2019/hash/b51a15f382ac914391a58850ab343b00-Abstract.html>.

927

928 Zhonghui You, Kun Yan, Jinmian Ye, Meng Ma, and Ping Wang. Gate decorator: Global filter
 929 pruning method for accelerating deep convolutional neural networks. In Hanna M. Wallach, Hugo
 930 Larochelle, Alina Beygelzimer, Florence d’Alché-Buc, Emily B. Fox, and Roman Garnett (eds.),
 931 *Advances in Neural Information Processing Systems 32: Annual Conference on Neural Information
 932 Processing Systems 2019, NeurIPS 2019, December 8-14, 2019, Vancouver, BC, Canada*, pp.
 933 2130–2141, 2019b. URL <https://proceedings.neurips.cc/paper/2019/hash/b51a15f382ac914391a58850ab343b00-Abstract.html>.

934

935 Ruichi Yu, Ang Li, Chun-Fu Chen, Jui-Hsin Lai, Vlad I. Morariu, Xintong Han, Mingfei
 936 Gao, Ching-Yung Lin, and Larry S. Davis. NISP: pruning networks using neuron im-
 937 portance score propagation. In *2018 IEEE Conference on Computer Vision and Pattern
 938 Recognition, CVPR 2018, Salt Lake City, UT, USA, June 18-22, 2018*, pp. 9194–9203.
 939 Computer Vision Foundation / IEEE Computer Society, 2018. doi: 10.1109/CVPR.2018.
 940 00958. URL http://openaccess.thecvf.com/content_cvpr_2018/html/Yu_NISP_Pruning_Networks_CVPR_2018_paper.html.

941

942 Sixing Yu, Arya Mazaheri, and Ali Jannesari. Topology-aware network pruning using multi-stage
 943 graph embedding and reinforcement learning. In Kamalika Chaudhuri, Stefanie Jegelka, Le Song,
 944 Csaba Szepesvári, Gang Niu, and Sivan Sabato (eds.), *International Conference on Machine
 945 Learning, ICML 2022, 17-23 July 2022, Baltimore, Maryland, USA*, volume 162 of *Proceedings of
 946 Machine Learning Research*, pp. 25656–25667. PMLR, 2022. URL <https://proceedings.mlr.press/v162/yu22e.html>.

947

948 Manzil Zaheer, Satwik Kottur, Siamak Ravanbakhsh, Barnabás Póczos, Ruslan Salakhutdinov,
 949 and Alexander J. Smola. Deep sets. In Isabelle Guyon, Ulrike von Luxburg, Samy Ben-
 950 gio, Hanna M. Wallach, Rob Fergus, S. V. N. Vishwanathan, and Roman Garnett (eds.),
 951 *Advances in Neural Information Processing Systems 30: Annual Conference on Neural
 952 Information Processing Systems 2017, December 4-9, 2017, Long Beach, CA, USA*, pp.
 953 3391–3401, 2017. URL <https://proceedings.neurips.cc/paper/2017/hash/f22e4747dalaa27e363d86d40ff442fe-Abstract.html>.

954

955 Chenglong Zhao, Bingbing Ni, Jian Zhang, Qiwei Zhao, Wenjun Zhang, and Qi Tian. Varia-
 956 tional convolutional neural network pruning. In *IEEE Conference on Computer Vision and
 957 Pattern Recognition, CVPR 2019, Long Beach, CA, USA, June 16-20, 2019*, pp. 2780–2789.
 958 Computer Vision Foundation / IEEE, 2019. doi: 10.1109/CVPR.2019.00289. URL http://openaccess.thecvf.com/content_CVPR_2019/html/Zhao_Variational_Convolutional_Neural_Network_Pruning_CVPR_2019_paper.html.

959

960

961 Allan Zhou, Kaien Yang, Kaylee Burns, Adriano Cardace, Yiding Jiang, Samuel Sokota, J. Zico
 962 Kolter, and Chelsea Finn. Permutation equivariant neural functionals. In Alice Oh, Tris-
 963 tan Naumann, Amir Globerson, Kate Saenko, Moritz Hardt, and Sergey Levine (eds.), *Ad-
 964 vances in Neural Information Processing Systems 36: Annual Conference on Neural Infor-
 965 mation Processing Systems 2023, NeurIPS 2023, New Orleans, LA, USA, December 10 - 16,
 966 2023*, 2023a. URL http://papers.nips.cc/paper_files/paper/2023/hash/4e9d8aeeab6120c3c83ccf95d4c211d3-Abstract-Conference.html.

967

968 Allan Zhou, Kaien Yang, Yiding Jiang, Kaylee Burns, Winnie Xu, Samuel Sokota, J. Zico
 969 Kolter, and Chelsea Finn. Neural functional transformers. In Alice Oh, Tristan Nau-
 970 mann, Amir Globerson, Kate Saenko, Moritz Hardt, and Sergey Levine (eds.), *Advances
 971 in Neural Information Processing Systems 36: Annual Conference on Neural Infor-
 mation Processing Systems 2023, NeurIPS 2023, New Orleans, LA, USA, December 10 - 16,*

972 2023, 2023b. URL http://papers.nips.cc/paper_files/paper/2023/hash/f4757db82a02eea015670ecca605d5cc-Abstract-Conference.html.
973
974

975 Allan Zhou, Chelsea Finn, and James Harrison. Universal neural functionals. In Amir Globersons,
976 Lester Mackey, Danielle Belgrave, Angela Fan, Ulrich Paquet, Jakub M. Tomczak, and Cheng
977 Zhang (eds.), *Advances in Neural Information Processing Systems 38: Annual Conference on
978 Neural Information Processing Systems 2024, NeurIPS 2024, Vancouver, BC, Canada, December
979 10 - 15, 2024*, 2024. URL http://papers.nips.cc/paper_files/paper/2024/hash/bd20595c8e5802ba40ed418f4ec116f0-Abstract-Conference.html.
980

981 Tao Zhuang, Zhixuan Zhang, Yuheng Huang, Xiaoyi Zeng, Kai Shuang, and Xiang Li. Neuron-level
982 structured pruning using polarization regularizer. In Hugo Larochelle, Marc'Aurelio Ranzato, Raia
983 Hadsell, Maria-Florina Balcan, and Hsuan-Tien Lin (eds.), *Advances in Neural Information Pro-
984 cessing Systems 33: Annual Conference on Neural Information Processing Systems 2020, NeurIPS
985 2020, December 6-12, 2020, virtual*, 2020. URL <https://proceedings.neurips.cc/paper/2020/hash/703957b6dd9e3a7980e040bee50ded65-Abstract.html>.
986

987 Zhuangwei Zhuang, Mingkui Tan, Bohan Zhuang, Jing Liu, Yong Guo, Qingyao Wu, Junzhou Huang,
988 and Jin-Hui Zhu. Discrimination-aware channel pruning for deep neural networks. In Samy Bengio,
989 Hanna M. Wallach, Hugo Larochelle, Kristen Grauman, Nicolò Cesa-Bianchi, and Roman Garnett
990 (eds.), *Advances in Neural Information Processing Systems 31: Annual Conference on Neural
991 Information Processing Systems 2018, NeurIPS 2018, December 3-8, 2018, Montréal, Canada*,
992 pp. 883–894, 2018. URL <https://proceedings.neurips.cc/paper/2018/hash/55a7cf9c71f1c9c495413f934dd1a158-Abstract.html>.
993

994

995

996

997

998

999

1000

1001

1002

1003

1004

1005

1006

1007

1008

1009

1010

1011

1012

1013

1014

1015

1016

1017

1018

1019

1020

1021

1022

1023

1024

1025

1026 A COMPARISON WITH PRIOR WORKS

1028 Our framework is entirely new and fundamentally different from all prior works. In this section, we
 1029 will compare our method with earlier ones to help you better understand the relationship between our
 1030 method and prior ones, and realize our unique innovations and advantages.

1032 A.1 GENERAL COMPARISON

1034 Previous pruning approaches can be broadly categorized into fixed pruning methods and learning
 1035 to prune methods. Our approach falls into the learning to prune category but learns in a completely
 1036 different way. For clarity, we provide a detailed comparison in Table 6 to help you better understand
 1037 how our work relates to previous studies.

1039 Table 6: Our framework is entirely new and has many advantages over previous works

	Fixed pruning	Learning to prune	Ours
Definition	Pruning with fixed hand-crafted algorithms.	Using neural network learning techniques to learn how to prune.	Also learning to prune, but learning in a completely different way.
Performance	Bad. Networks are complex and hand-crafted algorithms are quite limited	Good.	Good (almost best according to our experiments).
Cost	Low. No special extra training needed.	High. Need special extra training during each pruning.	Need special extra training before pruning. But once the training is done, can prune as many networks as we want without any special extra training.
Potential	Has already been well-studied and commonly used.	The pruning process is too tricky and costly. Can only be used in a very specific situation and lack of generality.	The pruning process is relatively more efficient. Can theoretically be used in almost all situations and has great generality.

1062 A.2 COMPUTATIONAL AND MEMORY COSTS

1064 One important question for almost all previous meta-learning approaches is the computational and
 1065 memory costs are too large. We provide some estimate of memory and computational costs for
 1066 scaling our methods to larger models and compare with two classic pruning methods–pruning at
 1067 initialization methods (cheap pruning, hard to train and low accuracy like Lee et al. (2019); Wang
 1068 et al. (2022)) and iterative magnitude pruning (costly, pruning during training and high performance
 1069 like Frankle & Carbin (2019); Molchanov et al. (2019)). The results show that our method achieves
 1070 outstanding results while uses relatively low costs.

1071 For convenience in expression, we refer to pruning at initialization as “init pruning”, iterative
 1072 magnitude pruning as “iter pruning” and our method as “meta pruning”.

1073 For all usual networks which satisfy Edge Number \gg Neuron Number, the memory and
 1074 computational cost are all $O(E)$ (E = Edge Number). This is obvious for init and iter pruning. For
 1075 meta pruning, our metanetwork doesn’t scale with the network. So all computation and memory cost
 1076 is it still $O(E)$.

1078 **PS:** The reason why our metanetwork doesn’t scale with the network is that it only learns how to
 1079 change weights based on local architectures and weights (the range of “local” is fixed for network of
 different sizes). In all our experiments, it is a small network compared to the to be pruned network,

1080 and it works well. So we have the confidence that it shouldn't and doesn't need to scale with the
 1081 networks.

1082 While all methods share the same asymptotic cost, their constant factors differ significantly.

1083 Computational cost breaks down as:

1085
$$\text{Compu Cost} = \text{Training cost} + \text{Pruning cost} + \text{Other cost}$$

1087

- **Init pruning:** Low training and pruning costs, negligible other cost.
- **Iter pruning:** High training cost (initial training + multiple finetuning steps) and high
 1088 pruning cost (multiple pruning rounds), no extra cost.
- **Meta pruning:** Moderate training cost (initial training + 3 finetuning steps), moderate
 1089 pruning cost (2 pruning steps), plus a small other cost consisting of metanetwork feedforward
 1090 and amortized meta-training cost per network.

1093

1094 We estimate the relative magnitude in the following table:

1095

1096

Computation	Training cost	Pruning cost	Other cost
Init	1T	1P	0
Iter	> 10T	> 5P	0
Meta	2–5T	2P	$\epsilon T + AT/N$

1100

1101 Where:

1102 T: Unit training cost

1103 P: Unit pruning cost

1104 ϵT : Metanetwork feedforward cost (almost zero compared to training cost)

1105 N: Number of networks pruned; meta-training cost is amortized over N (Once we get a metanetwork
 by meta-training, we can use it to prune as many networks as we want)

1106 A: Meta-training cost. A is estimated 5–20.

1107 Memory cost depends on both the amount of memory used and the duration of usage:

1108

Method	Amount	Duration	All
Init	Small	Short	Low
Iter	Medium	Long	Large
Meta	Large for a very short time, Small rest of the time	Medium	Medium but requires high memory capacity

1109

- **Init pruning:** Low memory usage for a short time.
- **Iter pruning:** Medium memory usage for a very long time.
- **Meta pruning:** The “feed forward through metanetwork” process requires large memory
 1110 usage but takes a very short time. For the rest of the time it uses little memory. It is faster
 1111 than iter pruning but slower than init pruning. While the average memory cost is moderate,
 1112 peak usage demands high memory capacity.

1113

1114 Meta-training requires large memory usage for a long time. But its cost can be amortized into
 1115 each pruning like we mentioned before. Take pruning resnet50 or ViT on ImageNet as example
 1116 (which is already quite large model and dataset), NVIDIA A100 with 80GiB VRAM is enough for
 1117 meta-training and feedforward through metanetwork and the rest training and finetuning can be done
 1118 on NVIDIA RTX 4090 with 24 GiB VRAM. When we don't have enough memory capacity, we can
 1119 also change the batch size and use more time to make up for the lack of our memory capacity.

1120

1121 In summary, our method achieves outstanding results while uses relatively low costs.

1122

1123 A.3 GENERALITY

1124

1125 Almost all previous meta-learning based pruning approaches, such as Liu et al. (2019); Li et al.
 1126 (2020); Wu et al. (2024), are tailored to a specific network and thus lack generality. Because of this
 1127 they require specialized training for each pruning instance.

1134 Unlike prior methods, our metanetwork learns a universal rule for adapting weights based on local
 1135 information, thereby enabling more effective pruning without relying on layer-specific or architecture-
 1136 specific heuristics. We need no special training during each pruning. Once our metanetwork is
 1137 trained, it can be used to prune as many networks as we want, and even transfer between datasets and
 1138 architectures.

1139 We divided the generality of learning to prune methods into 4 stages.

1140

- 1141 (1) Learning once prune one specific network.
- 1142 (2) Learning once prune one type of networks(same architecture and dataset) as many as
 1143 we want.
- 1144 (3) Learning once prune one group of networks(similar architectures and datasets) as
 1145 many as we want.
- 1146 (4) Learning once prune any networks.

1147 Here learning refers to learn with extra trainings like gradient descent, reinforcement learning, etc.
 1148 Finetuning or other fixed rules processes are not included. As far as we know, all prior learning to
 1149 prune methods only reach stage (1). Our method reaches stage (3) and shows great improvement in
 1150 generality over prior works. Follow our ideas and pretrain the metanetwork on various networks and
 1151 datasets may provide a possible way to state (4), whether this will work requires further exploration
 1152 in the future.

1153 In summary, our method shows great improvement in generality over prior learning to prune methods.

1154 A.4 A CONCRETE EXAMPLE

1155 We provide a concrete example compared with prior works and report everything-time, hardware,
 1156 gpu memory, results, etc. to give readers a more intuitive understanding of our method.

1157 We compare our work with Fang et al. (2023) on pruning ResNet56 on CIFAR10. We choose Fang
 1158 et al. (2023) because we want to compare our work with learning to prune methods in recent years
 1159 that also have strong results like us. The best candidates are Fang et al. (2023) and Wu et al. (2024).
 1160 While Wu et al. (2024) is a pruning before training method, both Fang et al. (2023) and our work are
 1161 pruning after training methods, so we choose Fang et al. (2023). The key idea of Fang et al. (2023) is
 1162 sparsity training before pruning. It does special training on the network before pruning to make it
 1163 more sparse and easier to prune.

1164 All experiments are run on 1 NVIDIA RTX 4090. See table 7 for time consumptions of different
 1165 methods. To align with Fang et al. (2023), we don't use init pruning, and target at a speed up of
 1166 2.5x, which is the largest speed up in paper Fang et al. (2023). In ours(full), we finetune 100 epochs
 1167 after metanetwork and 100 epochs after pruning. But later we found our method is stronger and
 1168 the speed up 2.5x isn't that hard. So in ours(efficient), we finetune 60 epochs after metanetwork
 1169 and 60 epochs after pruning but also get results comparable to Fang et al. (2023). The DepGraph
 1170 experiments use their default settings, sparsity training 100 epochs before pruning and finetune 100
 1171 epochs after pruning.

1172 Table 7: Time (minutes)

Process	Ours(full)	Ours(efficient)	DepGraph
Meta-Train	$192 + 165 = 357$	$192 + 165 = 357$	0
Prune & Finetune	67	43	84

1173 From the results we can see our methods is quite efficient. It uses 357 minutes for meta-train, which is
 1174 in a resonable range. We can greatly reduce time consumption in this process with some experiences,
 1175 but for the sake of fairness in comparison, we must pretend we have no relevant experience. Among
 1176 the 357 minutes, 192 minutes are used for generating 100 epochs metanetworks and 165 minutes
 1177 are used for visualizing the Acc VS. Speed Up Curve to select the appropriate metanetwork for
 1178 pruning. Once a metanetwork is trained, it can be used to prune as many networks as we want,

1188 so we can amortize the time for meta-training into each pruning. Figure 8 shows the amortized
 1189 time consumption of our work compared to DepGraph. In all, our work is more powerful and more
 1190 efficient in time if we prune several more networks or already have a trained metanetwork.
 1191
 1192

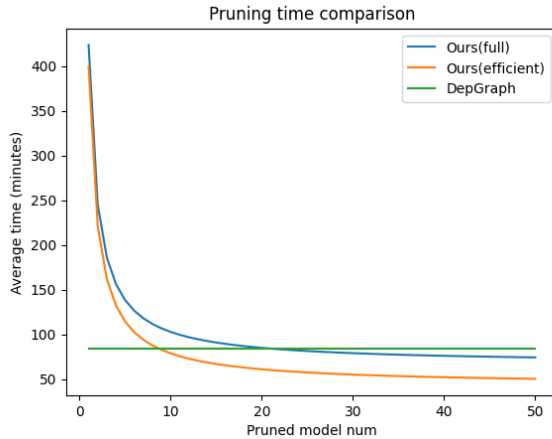


Figure 8: Amortized Time Consumption

1210 As we mentioned in section A.2, our methods use a large VRAM for a long time in meta-training, a
 1211 still large but relatively smaller VRAM for a very short time when feed forward through metanetwork
 1212 during pruning, and a small VRAM for the standard finetuning. Specifically in this experiment, we
 1213 use 10000 MiB for meta-training, 6000 MiB for feedforward through metanetwork, and 1000 MiB
 1214 for finetuning. NVIDIA A100 with 80 GiB VRAM is enough for meta-training large models like
 1215 ResNet50 and ViT-B-16. When we don't have enough memory capacity, we can also change the batch
 1216 size and use more time to make up for the lack of our memory capacity. We've also tried reducing
 1217 the size of metanetwork and fit on NVIDIA A100 40G and the results seem not much influenced.
 1218 All finetuning are standard finetuning and can be done on NVIDIA RTX 4090 with 24G VRAM.
 1219 In all, during pruning only the feed forward through metanetwork requires large VRAM for a very
 1220 short time and anything else is plain finetuning and requires small VRAM, during meta-training the
 1221 VRAM is in a resonable range.

1242 **B FRAMEWORK IMPLEMENTATION DETAILS**
 1243

1244 **B.1 METANETWORK(GNN) ARCHITECTURE**
 1245

1246 We build our metanetwork based on the message passing framework (Gilmer et al., 2017) and PNA
 1247 (Corso et al., 2020) architecture.

1248 Notation:

1249 $a \leftarrow b$: assignment/update, overwrite a with the value of b (10)

1250 $X \odot Y$: Hadamard/elementwise product, $(X \odot Y)_i = X_i Y_i$ (11)

1252 We use v_i to represent node i 's feature vector, and e_{ij} to represent feature vector of the edge between
 1253 i and j . We consider undirected edges, i.e., e_{ij} is the same as e_{ji} . Our metanetwork is as follows.

1255 First, all input node and edge features are encoded into the same hidden dimension.

1256 $v \leftarrow \text{MLP}_{\text{NodeEnc}}(v^{in})$, (12)

1258 $e \leftarrow \text{MLP}_{\text{EdgeEnc}}(e^{in})$. (13)

1259 Then they will pass through several message passing layers. In each layer, we generate the messages:

1261 $m_{ij} \leftarrow \text{MLP}_{\text{Node}}^1(v_i) \odot \text{MLP}_{\text{Node}}^2(v_j) \odot e_{ij}$, (14)

1262 $m'_{ij} \leftarrow \text{MLP}_{\text{Node}}^1(v_j) \odot \text{MLP}_{\text{Node}}^2(v_i) \odot (e_{ij} \odot \text{EdgeInvertor})$, (15)

1264 where m_{ij} and m'_{ij} respectively encode message from i to j and message from j to i , and EdgeInvertor
 1265 is defined as:

1266 $\text{EdgeInvertor} \triangleq [1, \underbrace{1, \dots, 1}_{\text{hidden_dim}/2}, \underbrace{-1, -1, \dots, -1}_{\text{hidden_dim}/2}]$. (16)

1268 The intuition behind EdgeInvertor is to let the first half dimensions to learn undirectional features
 1269 invariant to exchanging i, j , and the second half to capture directional information that changes
 1270 equivariantly with reverting i, j . Empirically we found this design the most effective among various
 1271 ways to encode edge features.

1272 Then, we aggregate the messages to update node features:

1274 $v_i \leftarrow v_i + \text{PNA}_{\text{Aggr}}(m_{ij}) + \text{PNA}_{\text{Aggr}}(m'_{ij})$, (17)

1275 where we have

1277 $\text{PNA}_{\text{Aggr}}(m_{ij}) \triangleq \text{MLP}_{\text{Aggr}} \left(\left[\text{MEAN}_{(i,j) \in E}(m_{ij}), \text{STD}_{(i,j) \in E}(m_{ij}), \text{MAX}_{(i,j) \in E}(m_{ij}), \text{MIN}_{(i,j) \in E}(m_{ij}) \right] \right)$. (18)

1280 For edge features in each layer, we also update them by:

1281 $e_{ij} \leftarrow e_{ij} + \text{MLP}_{\text{Edge}}^1(v_i) \odot \text{MLP}_{\text{Edge}}^2(v_j) \odot e_{ij}$
 1282 $+ \text{MLP}_{\text{Edge}}^1(v_j) \odot \text{MLP}_{\text{Edge}}^2(v_i) \odot (e_{ij} \odot \text{EdgeInvertor})$. (19)

1284 Finally, we use a decoder to recover node and edge features to their original dimensions:

1286 $v_{\text{pred}} \leftarrow \text{MLP}_{\text{NodeDec}}(v)$, (20)

1287 $e_{\text{pred}} \leftarrow \text{MLP}_{\text{EdgeDec}}(e)$. (21)

1289 We multiply predictions by a residual coefficient and add them to the original inputs as our final
 1290 outputs:

1291 $v_{\text{out}} = \alpha \cdot v_{\text{pred}} + v_{\text{in}}$, (22)

1293 $e_{\text{out}} = \beta \cdot e_{\text{pred}} + e_{\text{in}}$, (23)

1294 where α and β in practice are set to a small real numbers like 0.01. This design enables the
 1295 metanetwork to learn only the delta weights on top of the original weights, instead of a complete
 1296 reweighting.

1296

B.2 PRUNING CRITERION

1297

1298

B.2.1 DEPGRAPH AND TORCH-PRUNING

1299

1300

DepGraph (Fang et al., 2023) proposes a general sparsity regularization based structural pruning framework that can be applied to a wide range of neural network architectures, including CNNs, RNNs, GNNs, Transformers, etc. Alongside the paper, the authors released **Torch-Pruning**, a powerful Python library that enables efficient structural pruning for most modern architectures. In our work, the pruning criterion is designed based on the methodology of DepGraph (Fang et al., 2023), and all pruning operations are implemented using Torch-Pruning.

1305

1306

1307

1308

1309

1310

1311

1312

1313

1314

1315

1316

1317

1318

1319

1320

1321

1322

1323

Figure 9: A picture from (Fang et al., 2023). It shows how we group parameters together in structural pruning.

1324

B.2.2 STRUCTURAL PRUNING

1325

1326

1327

We perform most of our experiments by default using structural pruning, but also include a small number of experiments with unstructured and N:M sparsity pruning to demonstrate that our method can be applied to all kinds of pruning. Here we mainly introduce the structural pruning.

1328

1329

1330

1331

Structural pruning involves removing parameters in predefined *groups*, so that the resulting pruned model can be used as a standalone network—without relying on the original model with masks, nor requiring specialized AI accelerators or software to realize reductions in memory footprint and computational cost.

1332

1333

1334

1335

1336

1337

1338

1339

In structural pruning, a *pruning group* consists of all parameters that must be pruned together to maintain network consistency. For example, in Figure 9(a), if an input channel of convolution layer f_4 is pruned, the corresponding channel in batch normalization (BN) layer f_2 and the output channel of convolution layer f_1 must be pruned as well. Furthermore, due to the presence of a residual connection, the corresponding channels in BN layer f_5 and the output channel of convolution layer f_4 must also be removed. All of these channels together form a single pruning group. We define the *number of prunable dimensions* of a group as the size of the input channel dimension of Conv f_4 (which is equivalent to the corresponding dimensions in BN f_2 , the output channel of Conv f_1 , etc.)

1340

1341

For a more comprehensive theory to find all pruning groups in structural pruning, refer to the DepGraph (Fang et al., 2023) paper (section 3.1 & 3.2).

1342

1343

B.2.3 A IMPORTANCE SCORE FUNCTION

1344

1345

1346

1347

1348

1349

Given a parameter group $g = \{w_1, w_2, \dots, w_{|g|}\}$ with K prunable dimensions indexed by $w_t[k]$ ($t \in \{1, 2, \dots, |g|\}$), the score of the k th prunable dimension in group g is written as $I_{g,k}$, we introduce a general way to generate a series types of importance scores. The way has two key concepts, REDUCE and NORMALIZE. We first use REDUCE to reduce scores of parameters in the same group and in the same prunable dimension into one score.

$$I_{t,k} = \text{REDUCE}_{t:t \in \{1, 2, \dots, |g|\}} (|w_t[k]|^p) \quad (24)$$

1350 Here p is a hyperparameter and we usually set it to 2, REDUCE can be (but is not limited to) the
 1351 following:
 1352

- 1353 (1) **MEAN:** $(w_1 + w_2 + \dots + w_{|g|})/|g|$
- 1354 (2) **FIRST:** w_1

1355 Then we use NORMALIZE to normalize scores in the different prunable dimensions of the same
 1356 pruning group.
 1357

$$\hat{I}_{g,k} = I_{g,k} / \text{NORMALIZE}_{k:k \in \{1, 2, \dots, K\}}(I_{g,k}) \quad (25)$$

1360 Here NORMALIZE can be (but is not limited to) the following:
 1361

- 1362 (1) **NONE:** 1 (use no normalize).
- 1363 (2) **MEAN:** $(I_{g,1} + I_{g,2} + \dots + I_{g,K})/K$
- 1364 (3) **MAX:** The maximum among $I_{g,1}, I_{g,2}, \dots, I_{g,K}$

1365 We calculate scores of all prunable dimensions in all groups in a network, rank them and prune
 1366 according to their scores from lower to higher.
 1367

1368 B.2.4 A SPARSITY LOSS

1370 During training, our sparsity loss is defined as :

$$\mathcal{R}(g, k) = \sum_{k=1}^K \gamma_k \cdot \hat{I}_{g,k} \quad (26)$$

1375 Where γ_k refers to a shrinkage strength applied to the parameters to modify the gradients for better
 1376 training. Defined as :

$$\gamma_k = 2^{\frac{\alpha \sqrt{I_g^{\max}} - \sqrt{I_{g,k}}}{\sqrt{I_g^{\max}} - \sqrt{I_g^{\min}}}} \quad (27)$$

1379 Here α can be but is not limited to:
 1380

- 1381 (1) **4:** What we use as default in all our experiments.
- 1382 (2) **0:** Same as using no shrinkage strength.

1384 In sparsity loss, we treat γ_k and NORMALIZE in the denominator of $\hat{I}_{g,k}$ simply as constants, which
 1385 means gradients aren't backpropagated through them. Gradients only back propagated from $\mathcal{R}(g, k)$
 1386 to $I_{g,k}$ to the parameters of the network.

1387 In our code, rather than calculate the sparsity loss, we directly modify the gradients of the parameters
 1388 of the network, which get the same results.
 1389

1390 B.2.5 KINDS OF PRUNING CRITERION

1392 By choosing different ways of REDUCE and NORMALIZE (appendix B.2.3) and different α
 1393 (appendix B.2.4), we can make different pruning criteria in a uniform framework. **In most of our**
 1394 **experiments, we use MEAN REDUCE, MAX NORMALIZE, $\alpha = 4$, as our default pruning**
 1395 **criterion, and we name it group ℓ_2 norm max normalizer.** We also tried different criteria in
 1396 our experiments and found they are almost all effective, which further shows the flexibility and
 1397 effectiveness of our framework.

1398 B.2.6 PAY ATTENTION

1400 Though we draw ideas from Fang et al. (2023) and use their Torch-Pruning library, we find their
 1401 paper is inconsistent with their code. We wrote appendix B.2.3 & B.2.4 strictly based on their code,
 1402 which is the Torch-Pruning library. If you read the Fang et al. (2023) paper section 3.3, you may find
 1403 our description a little different from theirs, because their paper is inconsistent with their code, and
 we are in line with their code.

1404 **C EXPERIMENTAL PRELIMINARIES**

1405 **C.1 TERMINOLOGIES**

1406 **Speed Up:** In line with prior works, we define **Speed Up** \triangleq **Origin FLOPs / Pruned FLOPs**. It
 1407 reflects the extent to which our pruning reduces computation, thereby accelerating the network’s
 1408 operation.

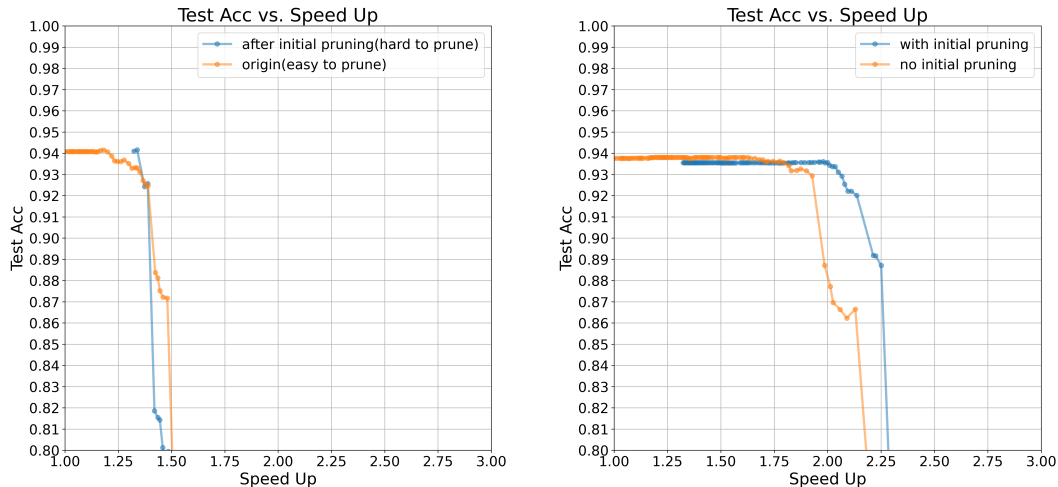
1409 **Acc vs. Speed Up Curve:** We generate the curve by prune the network little by little. After each
 1410 pruning step, we evaluated the model’s performance on the test set (no finetuning in this step) and
 1411 recorded a data point representing the current speed up and corresponding test accuracy. Connecting
 1412 these points forms a curve that illustrates how accuracy changes as the speed up increases.

1413 **C.2 PRUNING PIPELINE**

1414 Our pruning pipeline can be summarized as:

1415
$$\underbrace{\text{Initial Pruning (Finetuning)}}_{\text{Optional}} \rightarrow \underbrace{\text{Metanetwork (Finetuning)}}_{\text{Necessary}} \rightarrow \text{Pruning (Finetuning)} \quad (28)$$

1416 **Initial Pruning:** Empirically, we observe that the metanetwork performs better on hard to prune
 1417 origin networks. However, many networks are initially easy to prune. For instance, ResNet56
 1418 on CIFAR10 can be pruned with a $1.3 \times$ speedup and then finetuned without any accuracy loss.
 1419 Therefore, unless stated otherwise, we apply the initial pruning step in all our experiments—both
 1420 when generating meta-training data models and during pruning. In this step, we slightly prune the
 1421 original network with a fixed speed up (a hyperparameter that can be determined in a few quick trials)
 1422 to make it harder to prune without loss in accuracy (Figure 10a), thereby exploiting the full potential
 1423 of the metanetwork. This effect is analogous to removing low-quality samples from a dataset in order
 1424 to obtain a higher-quality subset: an easy to prune network contains many low-quality parameters,
 1425 which may harm the training of the metanetwork. This step isn’t necessary, but facilitates convergence,
 1426 saves VRAM use, and helps achieve better pruning results (Figure 10b) during most of the time.



1427 (a) The origin network is easy to prune, after initial
 1428 pruning and slight finetuning, it becomes hard
 1429 to prune.

1430 (b) Initial pruning helps get better metanetworks and
 1431 better pruning results

1432 Figure 10: With or without initial pruning (ResNet56 on CIFAR10 as an example)

1433 **Metanetwork:** Change the origin hard to prune network into a graph, feed it through the metanetwork
 1434 to get a new graph, and change it back into a new network.

1435 **Pruning:** Prune the new easy to prune network.

1458
1459 **Finetuning:** Train the network with a relatively small learning rate. This is a common step that is
1460 widely used in pruning tasks.
1461

1462 Unlike prior learning to prune methods that require special training during each pruning, our pruning
1463 pipeline only requires a feed forward through metanetwork and standard finetuning, which is simple,
1464 general and effective.
1465

1466 Once we have a metanetwork, we can prune as many networks as we want. All our pruning models are
1467 completely different from meta-training data models. This demonstrates our metanetwork naturally
1468 has great transferability and no prior work has done something like this before.
1469

1470

1471

1472

1473

1474

1475

1476

1477

1478

1479

1480

1481

1482

1483

1484

1485

1486

1487

1488

1489

1490

1491

1492

1493

1494

1495

1496

1497

1498

1499

1500

1501

1502

1503

1504

1505

1506

1507

1508

1509

1510

1511

1512 D EXPERIMENTAL ON CNNS
15131514
1515 D.1 GENERAL EXPERIMENT SETUP
15161517 D.1.1 GENERAL SETTINGS
15181519 **Optimizer:** For all data model training and fine-tuning, we use `torch.optim.SGD` with
1520 `momentum=0.9`. For meta-training, we employ `torch.optim.AdamW`. All learning rates
1521 are controlled using `torch.optim.lr_scheduler.MultiStepLR` with `gamma=0.1`. The
1522 learning rate is adjusted at specified milestones; for instance, if `milestones=[50, 90]`, the
1523 learning rate is multiplied by 0.1 at epochs 50 and 90. These settings are not strictly necessary—other
1524 optimizers and schedulers may be equally effective.1525 **Data for Meta-Training:** As discussed in Section 4.2, meta-training requires two types of data: data
1526 models and traditional training datasets. To generate a data model, we train a base model, perform
1527 initial pruning followed by finetuning, and finally save the model along with relevant information.
1528 Typically, generating 2–10 data models is sufficient, with 1–8 used for meta-training and the remainder
1529 reserved for meta-evaluation or testing.1530 **Meta Evaluation (Meta Eval):** Meta evaluation is a process used to assess the quality of the
1531 metanetwork during meta-training. **We did not include it in our final experiments due to its high**
1532 **computational cost; however, we retain it as an optional tool for future research.** At the end of
1533 each meta-training epoch, we evaluate the metanetwork by feeding unseen data models (not used in
1534 meta-training) through the network, finetuning, and then pruning to achieve the maximum speed-up
1535 while maintaining accuracy above a predefined threshold. A higher resulting speed-up indicates better
1536 metanetwork performance.1537 **Visualizing Metanetworks:** This is a key technique used throughout our experiments. When we
1538 refer to visualizing a metanetwork, we mean passing a model through the metanetwork, followed by
1539 finetuning, and then visualize the “Acc VS. Speed-Up” curve of the resulting model, as illustrated in
1540 Figure 5. This visualization provides insights into the metanetwork’s behavior and helps determine
1541 whether it is suitable for pruning. An ideal metanetwork should exhibit a long flat region in the
1542 curve where accuracy remains close to or above the target pruning accuracy. There are two ways
1543 to select a suitable metanetwork: (1) using meta-evaluation during meta-training, or (2) visualizing
1544 metanetworks post-training. In our final experiments, we exclusively use the second method, which
1545 is significantly more efficient. We typically do not visualize all metanetworks but instead search for
1546 the best one using a binary search strategy.1547 **Relationship between "Acc VS. Speed Up Curve" and Pruning Performance:** Empirically,
1548 pruning performance can be qualitatively predicted from the "Accuracy VS. Speed Up" curve. The
1549 accuracy in the flat region of the curve typically represents the maximum achievable accuracy; after
1550 pruning and finetuning, the final accuracy is usually the same or slightly lower, and sometimes only a
1551 little bit higher at most. The amount of speed up that preserves this top accuracy is generally larger
1552 than the speed up at the curve’s turning point, and these two values tend to correlate—the larger the
1553 turning point speed up, the larger the maintainable speed up. Therefore, if we aim for a pruned model
1554 with, for example, 93% accuracy, we should select a metanetwork whose flat-region accuracy is
1555 around or slightly above 93%, and whose flat region is as long as possible. We cannot give a theoretical
1556 guarantee between the "Acc VS. Speed Up" curve and the pruning performance. But this is not only
1557 our problem, because as far as we know, all other pruning methods can’t give theoretical guarantee
1558 between their pruning criterion and final performance as well. The reasons can be the network itself
1559 is too complex and processes like finetuning changes everything in an unpredictable way.1560 **Big Batch Size and Small Batch Size:** We use two different batch sizes in our experiments: a
1561 small batch size and a big batch size. The big batch size is used during meta-training to compute
1562 accuracy loss on new networks. Due to memory constraints, such large batches cannot be processed
1563 in a single forward and backward pass. Instead, we accumulate gradients over multiple smaller
1564 mini-batches before performing a single optimizer update—a common PyTorch practice. The big
1565 batch size is thus expressed as `batchsize * iters`, indicating that one `optimizer.step()`
1566 is performed after `iters` forward/backward passes, each using a mini-batch of size `batchsize`.
1567 For all other standard training and finetuning tasks, we use the small batch size.

1566
1567

D.1.2 GENERAL META TRAINING DETAILS

1568
1569
1570
1571
1572
1573
1574
1575
1576
1577

Equivalent Conversion between Network and Graph: During meta-training, we first convert the original network into an origin graph. Then, we feed this origin graph through the metanetwork to generate a new graph. Finally, we convert the new graph back into a new network. When converting the original network into the origin graph, all network parameters are mapped to either node or edge features in the graph. However, some graph features do not correspond to any network parameter. For these missing features, we use default values that effectively simulate the absence of those parameters. When converting the new graph back into the new network, we only map those trainable parameters from the new graph back to the new network. For untrainable parameters in the new network, we keep it the same as the old network. We provide more explanations for this conversion process in the following subsections: D.2, D.3, and D.4.

1578
1579
1580
1581

The Relative Importance of Sparsity Loss and Accuracy Loss: In our experiments, we introduce a hyperparameter called "pruner reg", which controls the relative importance of sparsity loss compared to accuracy loss. During backpropagation, the gradient from the sparsity loss is scaled(multiplied) by this "pruner reg" value, while the gradient from the accuracy loss remains unscaled.

1582
1583
1584
1585
1586
1587
1588
1589
1590

Meta Training Milestone: As discussed in the Ablation Study (Section 5.3), as the number of training epochs increases, the metanetwork's ability to make the network easier to prune becomes stronger, while its ability to maintain the accuracy becomes weaker. During meta-training, we usually set a milestone for our learning rate scheduler. Before this milestone, we use a relatively large learning rate to quickly improve the metanetwork's ability to make networks easier to prune. After the milestone, we switch to a smaller learning rate to finetune the metanetwork and slow down the change of the two abilities, allowing us to select a well-balanced metanetwork. To determine a reasonable milestone value, we can first perform a short meta-training phase using the large learning rate, then visualize the resulting metanetworks to identify the point where the accuracy-maintaining ability of metanetwork is a bit stronger than we expect.

1591
1592
1593
1594
1595
1596
1597
1598

Choose the Appropriate Metanetwork: During meta-training, we save the metanetwork after each epoch. After training is complete, we search for the most suitable metanetwork by visualizing its performance using a binary search strategy. Specifically, we start by visualizing the metanetwork from the middle epoch. If the accuracy of its flat region is below our target pruned accuracy, we next visualize the metanetwork from the first quarter of training. Otherwise, we check the one from the third quarter. We continue this process iteratively until we find a metanetwork that meets our criteria: a relatively high accuracy in the flat region and a long flat region indicating robustness to pruning.

1599
1600

D.1.3 GENERAL PRUNING DETAILS :

1601
1602
1603
1604
1605
1606
1607
1608
1609
1610
1611
1612
1613
1614
1615
1616
1617
1618
1619

Pruning Speed Up: Once a suitable metanetwork has been selected for pruning, the next step is to determine the target speed up. In general, after visualizing the metanetwork, we observe a flat region followed by a sharp decline in accuracy. We define a *turning point* as the speed up at which the accuracy drops below a certain threshold. Experimentally, we find that we can safely prune the model at a speed up slightly higher than this turning point without incurring any accuracy loss after finetuning. For instance, when pruning ResNet-56 on CIFAR-10, we consider an accuracy drop below 0.93 as the turning point (typically around $2.0 \times$ speed up), and in practice, we are able to achieve a $2.9 \times$ speed up with almost no loss in accuracy after finetuning.

1620
1621

D.2 RESNET56 ON CIFAR10

1622

D.2.1 EQUIVALENT CONVERSION BETWEEN NETWORK AND GRAPH

1623

We change ResNet56 into a graph with node features of 8 dimensions and edge features of 9 dimensions.

1624

The node features consist of 4 features derived from the batch normalization parameters (weight, bias, running mean, and running variance) of the previous layer, along with 4 features from the batch normalization of the previous residual connection. If no such residual connection exists, we assign default values [1, 0, 0, 1] to the corresponding 4 features.

1625

The edge features are constructed by zero-padding all convolutional kernels to a size of 3×3 (note that our networks only contain kernels of size 3×3 or 1×1), and then flattening them into feature vectors. We treat all residual connections as convolutional layers with kernel size 1×1 . For example, consider two layers A and B connected via a residual connection, with neurons indexed as $1, 2, 3, \dots$ in both layers. If the residual connection has no learnable parameters (i.e., it directly adds the input to the output), we represent the edge from A_i to B_i as a 1×1 convolutional kernel with value 1, and the edge from A_i to B_j (where $i \neq j$) as a 1×1 kernel with value 0. If the residual connection includes parameters (e.g., a downsample with a convolutional layer and batch normalization), we construct the edge features in the same way as for standard convolutional layers.

1626

D.2.2 META TRAINING

1627

Data Models : We generate 10 models as our data models, among them, 8 are used for meta-training and 2 are used for validation (visualize the metanetwork). When generating each data model, we train them 200 epochs with learning rate 0.1 and milestone "100, 150, 180", then pruning with speed up 1.32x, followed by a finetuning for 80 epochs with learning rate 0.01 and milestone "40, 70". Finally, we can get a network with accuracy around 93.5%.

1628

One Meta Training Epoch : Every epoch we enumerate over all 8 data models. When enumerate a data model, we feedforward it through the metanetwork and generate a new network. We feed all our CIFAR10 training data into the new network to calculate the accuracy loss, and use the parameters of new network to calculate the sparsity loss. Then we backward the gradients from both two losses to update our metanetwork.

1629

Training: We train our metanetwork with learning rate 0.001, milestone "3", weight decay 0.0005 and pruner reg 10. Finally we use metanetwork from epoch 39 as our final network for pruning.

1630

D.2.3 GPU USAGE

1631

All tasks can be run on 1 NVIDIA RTX 4090.

1632

D.2.4 FULL RESULTS

1633

All results are summarized in Table 8, where we repeat the pruning process 3 times using different seeds: 7, 8, 9. It is important to note that due to the design of our algorithm and implementation, we cannot prune the network to exactly the same speed up across different runs. For instance, when targeting a $1.3 \times$ speed up, the actual achieved speed up may be slightly larger, such as $1.31 \times$, $1.32 \times$, or $1.35 \times$.

1634

The aggregated statistical results are presented in Table 9, where each value is reported in the form of mean (standard deviation).

1635

D.2.5 HYPERPARAMETERS

1636

See Table 10.

1637

1638

1639

1640

Table 8: ResNet56 on CIFAR10 Full

Method	Base	Pruned	Δ Acc	Pruned FLOPs	Speed Up
NISP (Yu et al., 2018)	—	—	—	43.2%	1.76
Geometric (He et al., 2019b)	93.59	93.26	-0.33	41.2%	1.70
Polar (Zhuang et al., 2020)	93.80	93.83	0.03	46.8%	1.88
DCP-Adapt (Zhuang et al., 2018)	93.80	93.81	0.01	47.0%	1.89
CP (Li et al., 2017a)	92.80	91.80	-1.00	50.0%	2.00
AMC (He et al., 2018b)	92.80	91.90	-0.90	50.0%	2.00
HRank (Lin et al., 2020a)	93.26	92.17	-1.09	50.0%	2.00
SFP (He et al., 2018a)	93.59	93.36	-0.23	52.6%	2.11
ResRep (Ding et al., 2021)	93.71	93.71	0.00	52.8%	2.12
SCP (Kang & Han, 2020)	93.69	93.23	-0.46	51.5%	2.06
FPGM (He et al., 2019a)	93.59	92.93	-0.66	52.6%	2.11
FPC (He et al., 2020)	93.59	93.24	-0.35	52.9%	2.12
DMC (Gao et al., 2020)	93.62	92.69	-0.93	50.0%	2.00
GNN-RL (Yu et al., 2022)	93.49	93.59	0.10	54.0%	2.17
DepGraph w/o SL (Fang et al., 2023)	93.53	93.46	-0.07	52.6%	2.11
DepGraph with SL (Fang et al., 2023)	93.53	93.77	0.24	52.6%	2.11
ATO (Wu et al., 2024)	93.50	93.74	0.24	55.0%	2.22
Meta-Pruning (ours)	93.51	93.64	0.13	56.5%	2.30
Meta-Pruning (ours)	93.51	93.75	0.24	58.0%	2.38
Meta-Pruning (ours)	93.51	93.78	0.27	56.5%	2.30
GBN (You et al., 2019a)	93.10	92.77	-0.33	60.2%	2.51
AFP (Ding et al., 2018)	93.93	92.94	-0.99	60.9%	2.56
C-SGD (Ding et al., 2019)	93.39	93.44	0.05	60.8%	2.55
Greg-1 (Wang et al., 2021)	93.36	93.18	-0.18	60.8%	2.55
Greg-2 (Wang et al., 2021)	93.36	93.36	0.00	60.8%	2.55
DepGraph w/o SL (Fang et al., 2023)	93.53	93.36	-0.17	60.2%	2.51
DepGraph with SL (Fang et al., 2023)	93.53	93.64	0.11	61.1%	2.57
ATO (Wu et al., 2024)	93.50	93.48	-0.02	65.3%	2.88
Meta-pruning (ours)	93.51	93.64	0.13	65.6%	2.91
Meta-pruning (ours)	93.51	93.28	-0.23	65.9%	2.93
Meta-pruning (ours)	93.51	93.49	-0.02	66.0%	2.94
Meta-pruning (ours)	93.51	93.27	-0.24	66.8%	3.01
Meta-pruning (ours)	93.51	93.10	-0.41	66.9%	3.02
Meta-pruning (ours)	93.51	93.52	0.01	67.0%	3.03

Table 9: ResNet56 on CIFAR10 Statistics

Pruned Accuracy	Pruned FLOPs	Speed Up
93.72(± 0.06)	57.0%(± 0.71 %)	2.3267(± 0.0377)
93.47(± 0.15)	65.83%(± 0.17 %)	2.9267(± 0.0125)
93.30(± 0.17)	66.90%(± 0.08 %)	3.0200(± 0.0081)

Table 10: ResNet56 on CIFAR10 Hyperparameters

Types	Name	Value
Compute Resources	GPU parallel	NVIDIA RTX 4090 No
Batch size	small batch size big batch size	128 500×100
Prepare Data Models	data model num epoch lr weight decay milestone	10 (8 + 2) 200 0.1 0.0005 "100, 150, 180"
Train From Scratch	speed up epoch lr weight decay milestone	1.32 80 0.01 0.0005 "40, 70"
Initial Pruning		
Finetuning		
Metanetwork	num layer hiddim in node dim in edge dim node res ratio edge res ratio	8 64 8 9 0.01 0.01
Meta Training	lr weight decay milestone pruner reg	0.001 0.0005 "3" 10
Final Pruning	metanetwork epoch speed up epoch lr weight decay milestone	39 2.3, 2.9, 3.0 100 0.01 0.0005 "60, 90"
Finetuning After Metanetwork	epoch lr weight decay milestone	140 0.01 0.0005 "80, 120"
Finetuning After Pruning		

1782 D.3 VGG19 ON CIFAR100
 1783
 1784 D.3.1 EQUIVALENT CONVERSION BETWEEN NETWORK AND GRAPH
 1785
 1786 We change VGG19 into a graph with node features of 5 dimensions and edge features of 9 dimensions.
 1787
 1788 **The node features** consist of 4 features derived from the batch normalization parameters (weight,
 1789 bias, running mean, and running variance) of the previous layer and 1 feature derived from the bias
 1790 of previous layer (0 if bias doesn't exist).
 1791
 1792 **The edge features** are constructed by zero-padding all convolutional kernels to a size of 3×3 (note
 1793 that our networks only contain kernels of size 3×3 or 1×1), and then flattening them into feature
 1794 vectors.
 1795
 1796 D.3.2 META TRAINING
 1797
 1798 **Data Models :** We generate 10 models as our data models, among them, 8 are used for meta-training
 1799 and 2 are used for validation (visualize the metanetwork). When generating each data model, we
 1800 train them 200 epochs with learning rate 0.1 and milestone "100, 150, 180", then pruning with speed
 1801 up 2.0x, followed by a finetuning for 140 epochs with learning rate 0.01 and milestone "80, 120".
 1802 Finally, we can get a network with accuracy around 73.5%.
 1803
 1804 **One Meta Training Epoch :** Every epoch we enumerate over all 8 data models. When enumerate a
 1805 data model, we feedforward it through the metanetwork and generate a new network. We feed all our
 1806 CIFAR100 training data into the new network to calculate the accuracy loss, and use the parameters
 1807 of new network to calculate the sparsity loss. Then we backward the gradients from both two losses
 1808 to update our metanetwork.
 1809
 1810 **Training:** We train our metanetwork with learning rate 0.001, milestone "10", weight decay 0.0005
 1811 and pruner reg 10. Finally we use metanetwork from epoch 38 as our final network for pruning.
 1812
 1813 D.3.3 GPU USAGE
 1814
 1815 All tasks can be run on 1 NVIDIA RTX 4090.
 1816
 1817 D.3.4 FULL RESULTS
 1818
 1819 All results are summarized in Table 11, where we repeat the pruning process 3 times using different
 1820 seeds: 7, 8, 9. It is important to note that due to the design of our algorithm and implementation,
 1821 we cannot prune the network to exactly the same speed up across different runs. For instance, when
 1822 targeting a $8.90 \times$ speed up, the actual achieved speed up may be slightly larger, such as $8.95 \times$,
 1823 $9.01 \times$, or $9.02 \times$.
 1824
 1825 The aggregated statistical results are presented in Table 12, where each value is reported in the form
 1826 of mean (standard deviation).
 1827
 1828 D.3.5 HYPERPARAMETERS
 1829
 1830 See Table 13.
 1831
 1832
 1833
 1834
 1835

Table 11: VGG19 on CIFAR100 Full

Method	Base	Pruned	Δ Acc	Pruned FLOPs	Speed Up
OBD (Wang et al., 2019)	73.34	60.70	-12.64	82.55%	5.73
OBD (Wang et al., 2019)	73.34	60.66	-12.68	83.58%	6.09
EigenD (Wang et al., 2019)	73.34	65.18	-8.16	88.64%	8.80
Greg-1 (Wang et al., 2021)	74.02	67.55	-6.67	88.69%	8.84
Greg-2 (Wang et al., 2021)	74.02	67.75	-6.27	88.69%	8.84
DepGraph w/o SL (Fang et al., 2023)	73.50	67.60	-5.44	88.73%	8.87
DepGraph with SL (Fang et al., 2023)	73.50	70.39	-3.11	88.79%	8.92
Meta-Pruning (ours)	73.65	68.65	-5.00	88.81%	8.94
Meta-Pruning (ours)	73.65	67.63	-6.02	88.96%	9.06
Meta-Pruning (ours)	73.65	69.75	-3.90	88.83%	8.95

Table 12: VGG19 on CIFAR100 Statistics

Pruned Accuracy	Pruned FLOPs	Speed Up
68.68(± 0.87)	88.87%($\pm 0.07\%$)	8.9833(± 0.0544)

Table 13: VGG19 on CIFAR100 Hyperparameters

Types	Name	Value
Compute Resources	GPU parallel	NVIDIA RTX 4090 No
Batch size	small batch size big batch size	128 500×100
Prepare Data Models	data model num epoch lr weight decay milestone	10 (8 + 2) 200 0.1 0.0005 "100, 150, 180"
Train From Scratch	speed up epoch lr weight decay milestone	2.0 140 0.01 0.0005 "80, 120"
Initial Pruning		
Finetuning		
Metanetwork	num layer hiddim in node dim in edge dim node res ratio edge res ratio	8 32 5 9 0.05 0.05
Meta Training	lr weight decay milestone pruner reg	0.001 0.0005 "10" 10
Final Pruning	metanetwork epoch speed up epoch lr weight decay milestone	38 8.90 2000 0.01 0.0005 "1850, 1950"
Finetuning After Metanetwork	epoch lr weight decay milestone	2000 0.01 0.0005 "1850, 1950"
Finetuning After Pruning		

1944
1945

D.4 RESNET50 ON IMAGENET

1946
1947

D.4.1 EQUIVALENT CONVERSION BETWEEN NETWORK AND GRAPH

1948
1949
1950

We change ResNet50 into a graph with node features of 8 dimensions and edge features of 1, 9 or 49 dimensions. We employ 3 linear layers to project edge features of these 3 different dimensions into the same hidden dimension, enabling their integration into our graph neural network.

1951
1952
1953
1954

The node features consist of 4 features derived from the batch normalization parameters (weight, bias, running mean, and running variance) of the previous layer, along with 4 features from the batch normalization of the previous residual connection. If no such residual connection exists, we assign default values $[1, 0, 0, 1]$ to the corresponding 4 features.

1955
1956
1957
1958
1959
1960
1961
1962
1963

The edge features are constructed by simply flatten convolutional kernels into feature vectors (We have convolutional kernels of size 1×1 , 3×3 or 7×7). We treat all residual connections as convolutional layers with kernel size 1×1 . For example, consider two layers A and B connected via a residual connection, with neurons indexed as $1, 2, 3, \dots$ in both layers. If the residual connection has no learnable parameters (i.e., it directly adds the input to the output), we represent the edge from A_i to B_i as a 1×1 convolutional kernel with value 1. Different from section D.2, to reduce the VRAM footprint of the program, we build no edges between A_i and B_j ($i \neq j$). If the residual connection includes parameters (e.g., a downsample with a convolutional layer and batch normalization), we construct the edge features in the same way as for standard convolutional layers.

1964
1965

D.4.2 META TRAINING

1966
1967
1968
1969
1970

Data Models : We generate 3 models as our data models, among them, 2 are used for meta-training and 1 are used for validation (visualize the metanetwork). When generating each data model, we finetune them based on the pretrained weights for 30 epochs with learning rate 0.01 and milestone "10", then pruning with speed up 1.2920x, followed by a finetuning for 60 epochs with learning rate 0.01 and milestone "30". Finally, we can get a network with accuracy around 76.1%.

1971
1972
1973
1974
1975
1976
1977
1978
1979
1980
1981

One Meta Training Epoch : We train with `torch.nn.parallel.DistributedDataParallel` (pytorch data parallel) across 8 gpus. Unlike in Section D.2 and Section D.3, at the beginning of each epoch, we evenly distribute different data models across the GPUs. For example, since we have two data models, we load one on four GPUs and the other on the remaining four GPUs. At each iteration, we forward all eight models (replicated across the 8 GPUs) through the metanetwork to generate eight new models. We then feedforward a large batch of ImageNet data, evenly distributed through these eight new models, to compute the accuracy loss. We also use the parameters of the eight new networks to compute the sparsity loss. Then we backward the gradients from both two losses to update our metanetwork. Each training epoch consists of (ImageNet data num / big batch size) iterations, meaning that one full pass over the entire ImageNet dataset when computing the accuracy loss is considered as one epoch .

1982
1983
1984

Training: We train our metanetwork with learning rate 0.01, milestone "2", weight decay 0.0005 and pruner reg 10. Finally we use metanetwork from epoch 12 as our final network for pruning.

1985

D.4.3 GPU USAGE

1986
1987
1988
1989

Meta-Training and feed forward through the metanetwork during pruning requires large VRAM and needs to be run on NVIDIA A100. All other training and finetuning can be run on NVIDIA RTX 4090. In practice, we use 8 gpus in parallel.

1990

D.4.4 FULL RESULTS

1991
1992
1993
1994
1995
1996
1997

All results are summarized in Table 14, where we repeat the pruning process 3 times. It is important to note that due to the design of our algorithm and implementation, we cannot prune the network to exactly the same speed up across different runs. For instance, when targeting a $2.3 \times$ speed up, the actual achieved speed up may be slightly larger, such as $2.31 \times$, $2.32 \times$, or $2.35 \times$.

The aggregated statistical results are presented in Table 15, where each value is reported in the form of mean (standard deviation) .

1998
1999

D.4.5 HYPERPARAMETERS

2000

See Table 16.

2001
2002

Table 14: ResNet50 on ImageNet Full

Method	Base Top-1(Top-5)	Pruned Top-1(Δ)	Pruned Top-5(Δ)	Pruned FLOPs
DCP (Zhuang et al., 2018)	76.01%(92.93%)	74.95%(-1.06%)	92.32%(-0.61%)	55.6%
CCP (Peng et al., 2019)	76.15%(92.87%)	75.21%(-0.94%)	92.42%(-0.45%)	54.1%
FPGM (He et al., 2019a)	76.15%(92.87%)	74.83%(-1.32%)	92.32%(-0.55%)	53.5%
ABCP (Lin et al., 2020b)	76.01%(92.96%)	73.86%(-2.15%)	91.69%(-1.27%)	54.3%
DMC (Gao et al., 2020)	76.15%(92.87%)	75.35%(-0.80%)	92.49%(-0.38%)	55.0%
Random (Li et al., 2022)	76.15%(92.87%)	75.13%(-1.02%)	92.52%(-0.35%)	51.0%
DepGraph (Fang et al., 2023)	76.15%(-)	75.83%(-0.32%)	-	51.7%
ATO (Wu et al., 2024)	76.13%(92.86%)	76.59% (+0.46%)	93.24% (+0.38%)	55.2%
DTP (Li et al., 2023)	76.13%(-)	75.55%(-0.58%)	-	56.7%
ours	76.14%(93.11%)	76.13%(-0.01%)	92.78%(-0.33%)	57.2%
ours	76.14%(93.11%)	76.24% (+0.20%)	93.09% (-0.02%)	57.1%
ours	76.14%(93.11%)	76.08%(-0.06%)	92.93%(-0.18%)	56.9%

2016

2017
2018

Table 15: ResNet50 on ImageNet Statistics

Pruned FLOPs (Speed Up)	Pruned Top-1	Pruned Top-5
57.1%(2.33 \times)	76.15%($\pm 0.07\%$)	92.93%($\pm 0.13\%$)

2019

2020

2021

2022

2023

2024

2025

2026

2027

2028

2029

2030

2031

2032

2033

2034

2035

2036

2037

2038

2039

2040

2041

2042

2043

2044

2045

2046

2047

2048

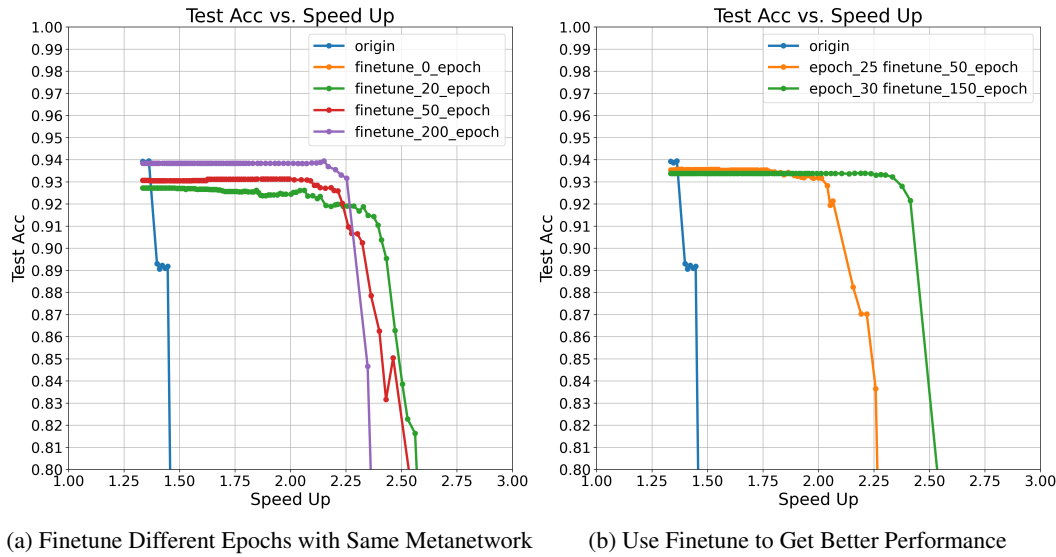
2049

2050

2051

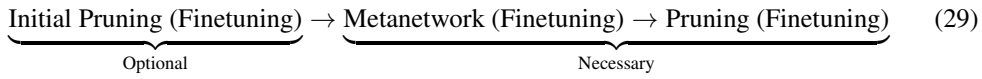
Table 16: ResNet50 on ImageNet Hyperparameters

Types	Name	Value
Compute Resources	GPU parallel	NVIDIA A100 & NVIDIA RTX 4090 8
Batch size	small batch size big batch size	32×8 $32 \times 8 \times 200$
Prepare Data Models Generate Data Model	data model num epoch lr weight decay milestone speed up epoch lr weight decay milestone	3 (2 + 1) 30 0.01 0.0001 "10" 1.2920 60 0.01 0.0001 "30"
Metanetwork	num layer hiddim in node dim node res ratio edge res ratio	6 16 8 0.002 0.002
Meta Training	lr weight decay milestone pruner reg	0.01 0.0005 "2" 10
Final Pruning Finetuning After Metanetwork	metanetwork epoch speed up epoch lr weight decay milestone epoch lr weight decay milestone	12 2.3095 200 0.01 0.0001 "120, 160, 185" 200 0.01 0.0001 "120, 160, 185"
Finetuning After Pruning		

2106 E MORE ABOUT ABLATION STUDY
21072108 E.1 FINETUNING AFTER METANETWORK
2109

2127 Figure 11: Finetune After Metanetwork (ResNet56 on CIFAR10 as example)

2130 As mentioned in section 5.1, our pruning pipeline can be summarized as:

2135 In this pipeline, finetuning after pruning is a common way to improve the accuracy. However,
2136 finetuning after the metanetwork is first proposed by us and may raise questions for readers regarding
2137 its impact on performance—whether it is necessary or beneficial? In this section, we aim to clarify the
2138 effects of finetuning after the metanetwork and demonstrate that it is both necessary and advantageous.2139 To illustrate this, we use the example of pruning ResNet56 on CIFAR10. In Figure 11a, we visualize
2140 the "Acc vs. Speed Up" curves for models after the same metanetwork and after various amounts
2141 of finetuning. Without any finetuning after the metanetwork, the network's accuracy is nearly zero
2142 (which is why there is no "finetune_0_epoch" line in the figure—it lies at the bottom). Directly
2143 proceeding to pruning and finetuning from such an unfinetuned network experimentally results in
2144 poor performance.2145 However, as we increase the number of finetuning epochs after the metanetwork, several interesting
2146 observations emerge:

- 2147 • **Quickly Recover:** The accuracy of our network after metanetwork quickly recovers after
2148 only very few finetuning, indicating that our metanetwork has the ability to preserve the
2149 accuracy (i.e. our accuracy loss in meta-training works)
- 2150 • **Trend of Change:** As the number of finetuning epochs increases, the flat portion of the
2151 curve becomes shorter or stays the same, and the overall accuracy of this region improves.

2153 When we feed the same network into metanetworks trained for different numbers of meta-training
2154 epochs and get several modified networks, then finetune them with different epochs to reach the same
2155 accuracy (as shown in Figure 11b), another important pattern emerges:

- 2157 • **More Finetune Better Performance :** A network obtained from a metanetwork with more
2158 meta-training epochs can typically achieve the same accuracy as one from a metanetwork
2159 with fewer meta-training epochs—but requires more finetuning. Importantly, the former
usually results in better pruning performance. This is evident in Figure 11b, where the green

2160 line (representing a higher meta-training epoch) exhibits a longer flat region, indicating
2161 improved robustness to pruning.
2162

2163 This suggests that the effectiveness of our method can be further improved by employing metanet-
2164 works trained for more meta-training epochs and applying more finetuning afterward. In practice,
2165 however, we avoid excessive finetuning in order to keep the number of finetuning epochs within a
2166 reasonable range, allowing for multiple experimental trials.

2167 Overall, all finetuning in our pipeline is necessary and effective.
2168
2169
2170
2171
2172
2173
2174
2175
2176
2177
2178
2179
2180
2181
2182
2183
2184
2185
2186
2187
2188
2189
2190
2191
2192
2193
2194
2195
2196
2197
2198
2199
2200
2201
2202
2203
2204
2205
2206
2207
2208
2209
2210
2211
2212
2213

2214 **F EXPERIMENTS ON TRANSFERABILITY**
22152216 **F.1 TRANSFER BETWEEN DATASETS**
22172218 The common pruning pipeline is:
2219

2220 Initial Pruning (Finetuning) → Metanetwork (Finetuning) → Pruning (Finetuning) (30)
2221

2222 Pruning pipeline for **None** is:
2223

2224 Initial Pruning (Finetuning) → Pruning (Finetuning) (31)
2225

2226 The dataset of a to be pruned network means we do all training and finetuning on it using this dataset.
2227 The dataset of a metanetwork means we generate dataset models, meta-train the metanetwork using
2228 this dataset.
22292230 We mainly have 2 hyperparameters here—*initial speed up* and *final speed up*. We approximately set
2231 them based on the difficulty of each dataset. Here dataset refers to the dataset of the to be pruned
2232 network (rows in Table 17). For CIFAR10, the initial pruning speed up is 1.32x and the final speed
2233 up is 3.0x. For CIFAR100 the initial pruning speed up is 1.32x and the final speed up is 2.5x. For
2234 SVHN, the initial pruning speed up is 3.0x and the final speed up is 10.0x.
22352236 **Table 17: Transfer between datasets:** All networks’ architecture is ResNet56. Columns represent
2237 the training datasets for the metanetwork, and rows represent the training datasets for the to be pruned
2238 network. “None” indicates using no metanetwork. Results with metanetwork is obviously better than
2239 no metanetwork (The only exception is when training datasets for the to be pruned network is SVHN,
2240 and we guess this is because the dataset SVHN itself is too easy).
22412242

Dataset\Metanetwork	CIFAR10	CIFAR100	SVHN	None
CIFAR10	93.35	92.47	92.87	91.28
CIFAR100	69.97	70.16	69.25	68.91
SVHN	96.79	96.50	96.86	96.78

2244 **F.2 TRANSFER BETWEEN ARCHITECTURES**
22452246 The common pruning pipeline is:
2247

2248 Initial Pruning (Finetuning) → Metanetwork (Finetuning) → Pruning (Finetuning) (32)
2249

2250 Pruning pipeline for **None** is:
2251

2252 Initial Pruning (Finetuning) → Pruning (Finetuning) (33)
2253

2254 The architecture of a to be pruned network means this network is constructed using this architecture.
2255 The architecture of a metanetwork means all dataset models we generated for meta-training this
2256 metanetwork use this architecture.
22572258 We mainly have 2 hyperparameters here—*initial speed up* and *final speed up*. We approximately set
2259 them based on the ability of each architecture. Here architecture refers to the architecture of the to be
2260 pruned network (rows in Table 18). For ResNet56, the initial pruning speed up is 1.32x and the final speed
2261 up is 3.0x. For ResNet110 the initial pruning speed up is 2.0x and the final speed up is 4.0x.
22622263 **F.3 TRANSFER FROM SMALL DATASET TO LARGE DATASET**
22642265 When we are using large dataset like imagenet, is it possible that we use a much smaller dataset
2266 during meta-training but get the same results? Our answer is yes.
22672268 When pruning Resnet50 on IMAGENET, we evenly choose 10% on each class in IMAGENET
2269 and form a new subset dataset. Meta-Training using this subset causes almost no drop in accuracy.
2270 See results in Table 19. This suggest that even 10% percent dataset is enough in meta-train to let
2271 metanetwork learn the pruning strategy.
2272

2268 **Table 18: Transfer between architectures.** All training dataset is CIFAR10. Columns represent
 2269 the architectures used for training the metanetwork, and rows represent the architectures of the to be
 2270 pruned network. “None” indicates using no metanetwork. All results with metanetwork is obviously
 2271 better than no metanetwork.

Architecture\Metanetwork	ResNet56	ResNet110	None
ResNet56	93.40	92.81	92.08
ResNet110	93.04	93.38	92.40

2277 **Table 19: During meta-train, use full ImageNet vs. only 10% ImageNet**

Method	Base Top-1(Top-5)	Pruned Top-1(Δ)	Pruned Top-5(Δ)	Pruned FLOPs
ours	76.14%(93.11%)	76.13%(-0.01%)	92.78%(-0.33%)	57.2%
ours(10%)	76.14%(93.11%)	76.24%(+0.10%)	92.65%(-0.46%)	57.0%

2285 F.4 TRANSFER FROM CLASSIFICATION TASK TO DETECTION TASK

2287 We transfer the metanetwork from a classification task into another detection task. The detection
 2288 dataset is PASCAL VOC 07 (Girshick et al., 2014). Our detection network is a Faster R-CNN
 2289 detector with an ImageNet-pretrained ResNet-50 backbone (conv layers only, no FPN), a single-scale
 2290 RPN with 5×3 anchors per location, RoIAlign to 7×7 , and the default torchvision Fast R-CNN
 2291 two-FC-layer head for 21-way VOC classification and bounding-box regression.

2292 We use metanetwork traind when pruning Resnet50 on ImageNet. During pruning, we prune the
 2293 resnet50 backbone with 2.5x speed up. Results are in Table 20. We can see that metanetwork does
 2294 help preserve the detection ability of the network even if it is trained on a classification task. This
 2295 is not a perfect experiment because nowadays there are much more different and stronger detection
 2296 architectures and pretrain is widely used to enhance the network’s ability. But adding too many
 2297 complex structures would make the experimental results difficult to analyze. So we conduct this
 2298 simple and fair experiment and it demonstrates that our metanetwork can transfer to different tasks.

2299 **Table 20: Transfer classification to detection**

Method	Origin	Prune w/o metanetwork	Prune with metanetwork
mAP	0.6061	0.4524	0.5173

2322 **G EXPERIMENTS ON TRANSFORMERS**

2323 **G.1 MHSA TO GRAPH**

2324 A MHSA (multi-head self-attention) begins with linear projections of the input \mathbf{X} using $3H$ independent weight matrices— \mathbf{H} each for queries, keys, and values. For each head $h \in 1, \dots, H$:

$$2329 \quad Q_h = \mathbf{X} \mathbf{W}_h^Q, \quad K_h = \mathbf{X} \mathbf{W}_h^K, \quad V_h = \mathbf{X} \mathbf{W}_h^V.$$

2331 Then each head computes attention via

$$2333 \quad Y_h = \text{softmax}(Q_h K_h^\top) V_h,$$

2334 The outputs Y_1, \dots, Y_H are concatenated and linearly projected:

$$2336 \quad \text{MHSA}(\mathbf{X}) = \text{Concat}(Y_1, \dots, Y_H) \mathbf{W}^O.$$

2338 The input and output are both d -dimensional. Each head produces d_H -dimensional outputs. When
2339 changing to a graph, we represent this with d input nodes in the first layer, $H \cdot d_H$ attention head
2340 nodes in the second layer, and d output nodes in the third layer.

2341 Between the first and the second layer, we model the three projection types (query, key, value) using
2342 multidimensional edge features: for each edge (i, j) in head h , the feature is
2343

$$2344 \quad e_{ij}^h = ((\mathbf{W}_h^Q)_{ij}, (\mathbf{W}_h^K)_{ij}, (\mathbf{W}_h^V)_{ij}).$$

2346 Between the second and third layer, concatenation and the final projection \mathbf{W}^O are handled naturally
2347 by the graph structure and treated as a standard linear layer.

2348 In summary, every pair of nodes between the first and second layers is connected by an edge
2349 characterized by three-dimensional features, which represent the attention parameters. Each pair of
2350 nodes between the second and third layers is connected by an edge with a single-dimensional feature,
2351 corresponding to the final linear projection.

2353 **G.2 EQUIVALENT CONVERSION BETWEEN NETWORK AND GRAPH**

2355 We change ViT-B/16 into a graph with node features of 6 dimensions and edge features of 1, 3 or 256
2356 dimensions. We employ 3 linear layers to project edge features of these 3 different dimensions into
2357 the same hidden dimension, enabling their integration into our graph neural network.

2358 **The node features** consist of 6 features, they are weight and bias of previous layer norm, bias
2359 of previous linear layer, biases of query, key, value of previous attention layer. In the case that
2360 any of these features doesn't exist, they are replaced by a default value of $[1, 0, 0, 0, 0, 0]$ at their
2361 corresponding positions.

2362 **The edge features** are constructed almost in the same way as previous experiments. The only new
2363 part is MHSA, and we construct it as described in Appendix G.1.

2365 **G.3 META TRAINING**

2367 **Data Models:** We use the default ViT-B/16 provided by PyTorch as the only data model. All training
2368 and pruning are conducted on this model, as training several separate models from scratch would be
2369 prohibitively time-consuming. Moreover, this choice ensures consistency with prior work in the field.
2370 Based on the Acc VS. speed up curve of the original ViT (Figure 12), we do initial pruning with a
2371 speed up of 1.0370x and apply no finetuning. This configuration yields a network with an accuracy
2372 of 81%.

2373 **One Meta Training Epoch :** The same as ResNet50 on ImageNet (Appendix D.4.2).

2374 **Training:** We train our metanetwork with learning rate 0.01, milestone "3", weight decay 0.0005
2375 and pruner reg 1000. Finally we use metanetwork from epoch 6 as our final network for pruning.

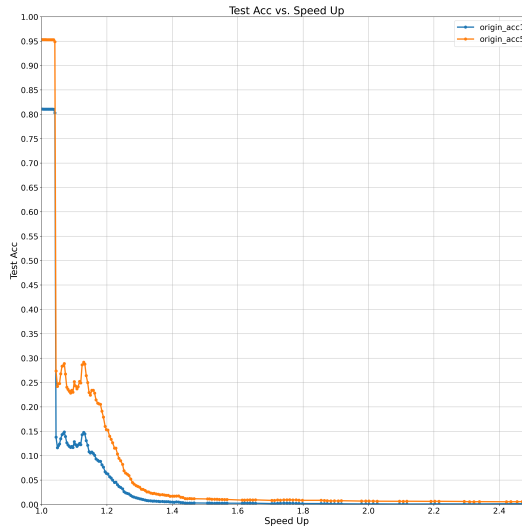


Figure 12: Acc VS. Speed Up curve of the origin ViT

2396 G.4 GPU USAGE

2398 Meta-Training and feed forward through the metanetwork during pruning requires large VRAM and
 2399 needs to be run on NVIDIA A100. All other training and finetuning can be run on NVIDIA RTX
 2400 4090. In practice, we use 8 gpus in parallel.

2401 G.5 FULL RESULTS

2403 All results are summarized in Table 21.

2405 G.6 HYPERPARAMETERS

2407 See Table 22.

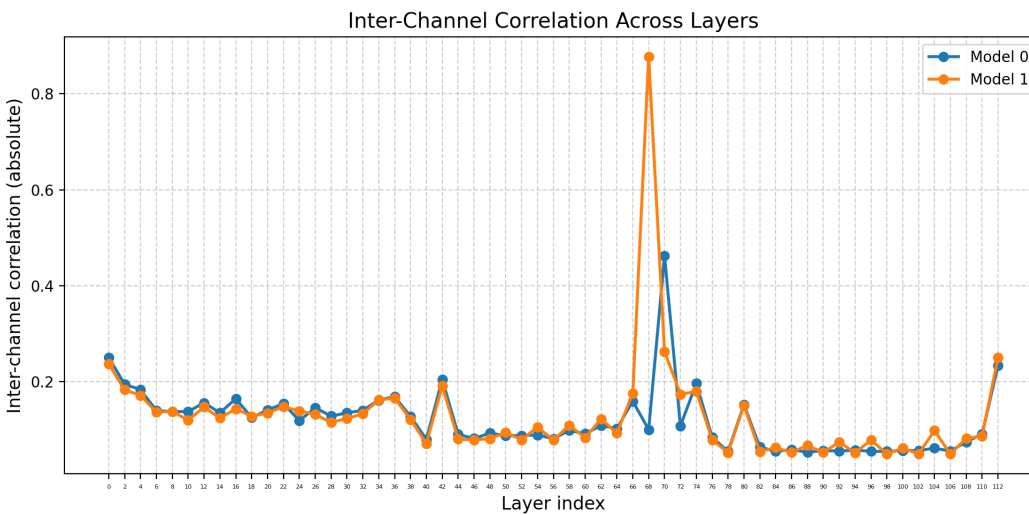
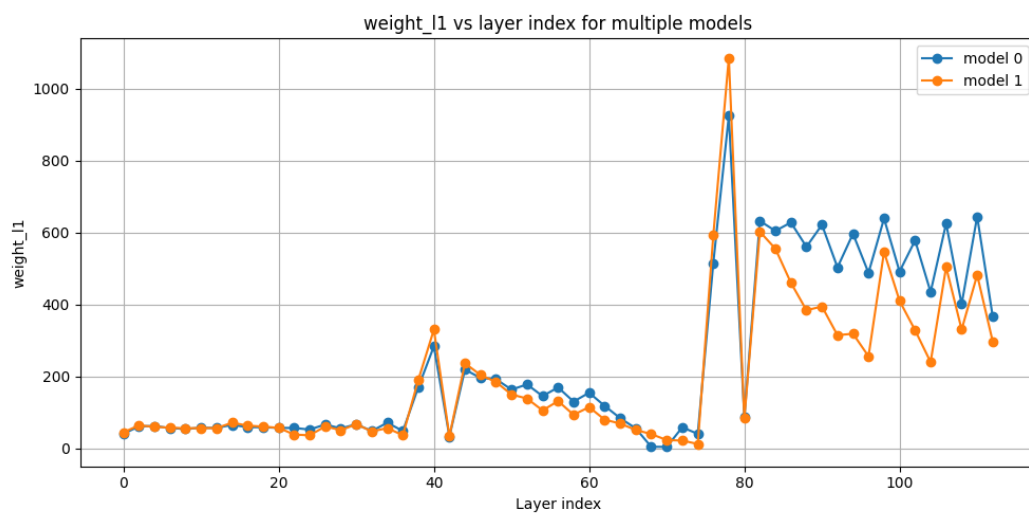
Table 21: ViT-B/16 on ImageNet

2411	Method	2412	Base Top-1	2413	Pruned Top-1	2414	Δ Acc	2415	FLOPs
2412	ViT-B/16 (Dosovitskiy et al., 2021)	2413	81.07%	2414	-	2415	-	2416	17.6
2413	CP-ViT (Song et al., 2022)	2414	77.91%	2415	77.36%	2416	-0.55%	2417	11.7
2414	DepGraph (Fang et al., 2023)	2415	81.07%	2416	79.17%	2417	-1.90%	2418	10.4
2415	MetaPruning(ours)	2416	81.07%	2417	78.26%	2418	-2.81%	2419	10.3

Table 22: ViT-B/16 on ImageNet Hyperparameters

Types	Name	Value
Compute Resources	GPU parallel	NVIDIA A100 & NVIDIA RTX 4090 8
Batch size	small batch size big batch size	128×8 $32 \times 8 \times 200$
Prepare Data Models Generate Data Model	data model num epoch lr weight decay milestone speed up	1 0 - - - 1.0370
Initial Pruning Finetuning	epoch lr weight decay milestone	0 - - -
Metanetwork	num layer hiddim in node dim node res ratio edge res ratio	3 4 6 0.1 0.1
Meta Training	lr weight decay milestone pruner reg	0.001 0.0005 - 10
Final Pruning Finetuning After Metanetwork	metanetwork epoch speed up epoch lr weight decay scheduler label smoothing mixup alpha cutmix alpha	22 1.7 300 0.01 0.01 cosineannealinglr 0.1 0.2 0.1
Finetuning After Pruning	epoch lr weight decay scheduler label smoothing mixup alpha cutmix alpha	100 0.0001 0.0001 cosineannealinglr 0.1 0.2 0.1

2430
2431
2432
2433
2434
2435
2436
2437
2438
2439
2440
2441
2442
2443
2444
2445
2446
2447
2448
2449
2450
2451
2452
2453
2454
2455
2456
2457
2458
2459
2460
2461
2462
2463
2464
2465
2466
2467
2468
2469
2470
2471
2472
2473
2474
2475
2476
2477
2478
2479
2480
2481
2482
2483

2484 H MORE VISUALIZATION OF STATISTICS
2485
2486
2487

2538
2539
2540
2541
2542
2543
2544
2545
2546
2547
2548
2549
2550
2551
2552
2553
2554
2555
2556
2557
2558
2559
2560
2561
2562
2563
2564
2565
2566
2567
2568
2569
2570
2571
2572
2573
2574
2575
2576
2577
2578
2579
2580
2581
2582
2583
2584
2585
2586
2587
2588
2589
2590
2591

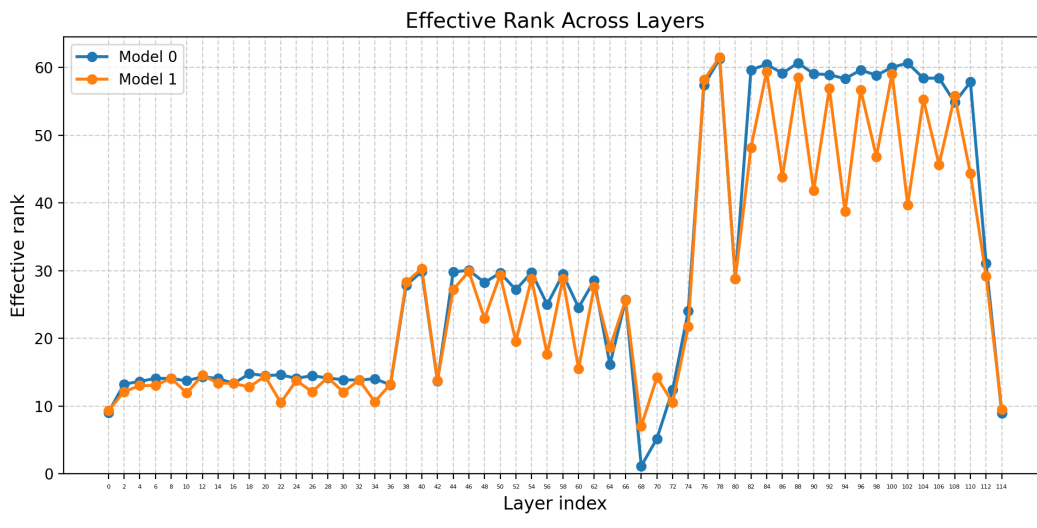


Figure 15: Efficient Rank

2592 **I THE USE OF LARGE LANGUAGE MODELS**

2593
2594 We only use LLMs to check grammar errors and polish our writing. All other works are done by
2595 human writers.

2596

2597

2598

2599

2600

2601

2602

2603

2604

2605

2606

2607

2608

2609

2610

2611

2612

2613

2614

2615

2616

2617

2618

2619

2620

2621

2622

2623

2624

2625

2626

2627

2628

2629

2630

2631

2632

2633

2634

2635

2636

2637

2638

2639

2640

2641

2642

2643

2644

2645